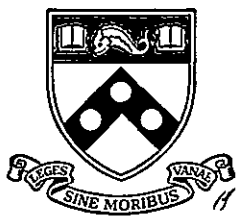

UNIVERSITY of PENNSYLVANIA

The Towne School
of
Civil and Mechanical Engineering

PHILADELPHIA, PENNSYLVANIA 19104

INSTITUTE FOR DIRECT ENERGY CONVERSION

TOWNE SCHOOL

UNIVERSITY OF PENNSYLVANIA

PHILADELPHIA, PENNSYLVANIA

RESEARCH FOR THE IMPROVEMENT OF SILICON SOLAR CELL EFFICIENCY

STATUS REPORT

SR 17

Period Covered: July 1, 1970 to December 31, 1970

Author: M. Wolf

NATIONAL AERONAUTICS AND SPACE ADMINISTRATION

GRANT NGL-39-010-001

JANUARY 1971

TABLE OF CONTENTS

Summary

The investigation into the interrelationships between material and dimensional parameters in their influence on collection efficiency from both the base region and the diffused region is completed. As a result, a set of curves constituting essentially a "silicon solar cell design handbook" could be issued. The essential results of this study are:

1) It is theoretically possible to collect over 99% of the minority carriers generated by photon absorption, even in thin solar cells.
2) A wide range of material and dimensional parameter combinations permits approaching the ideal case.
3) A diffusion length at least 3 times the thickness of the diffused region is required to fulfill point 2 above, but near 10 times the thickness is needed to satisfy point 1. In the base region a diffusion length of 300 μm is satisfactory.
4) Until diffusion length in the diffused region can be better controlled than at present, improvement has to be accomplished through thickness reduction.
5) Reduction of surface recombination velocity will be a necessity, but higher values can be tolerated than had been thought before.
6) Base region diffusion lengths, as achievable with present technologies, are sufficient from the collection efficiency viewpoint.
7) In the base region, the detrimental effect of the back contact can be neutralized by a drift field in front of the back contact. Its dimensions are not critical.
8) Longer minority carrier lifetimes will be wanted from the viewpoint of the IV-characteristic. Also, trade-offs may be required against collection efficiency considerations. This will be particularly true for point 7 above.

Recommendation:

Proceed in the project as planned. Beyond this, continue the general stress on improvement of low resistivity silicon material properties, and on reduction of surface recombination velocity.

I. Introduction

This progress report is the first semi-annual report on contract NGL-39-010-001, covering the period from July 1, 1970 to December 31, 1970. The object of the mentioned contract is research for the improvement of solar cell efficiency, primarily oriented towards silicon solar cells.

Most of the work during the first half year has concerned itself with deepening the understanding of the collection efficiency effects observed in present solar cells, and with establishing design criteria for future, improved silicon solar cells. This has been done on a theoretical basis, using previously published relationships and making use of the computer as an expedient tool for performing a quantity of design calculations which otherwise could not have been carried out because of the complexity of the computations.

The second part of the effort has been directed towards acquiring a similarly useful tool for the further investigation of the relationship governing the current-voltage characteristic of the silicon solar cells. For this purpose, a computer program has been developed to calculate the five parameters which determine the current-voltage characteristic of a silicon solar cell, based on the assumption that the characteristic is composed of two superimposed exponential terms including series resistance. In order to arrive at the best possible values of these five parameters, based on all the experimental data available for the characteristic of a given device the least squares method has been chosen as the basis for this program. The extent of the usefulness of the program will have to prove itself throug its future application.

The following three sections contain a discussion of the collection efficiency in the base region of silicon solar cells, the collection efficiency from the diffused region of silicon solar cells, and a discussion of the computer program for evaluation of the parameters of the current-voltage characteristic. Section V summarizes the status relative to the work schedule, while section VI lists the work planned for the next half year.

II. Collection Efficiency from the Base Region

1. Introduction

A considerable amount of work concerning the collection efficiency from the base region has been carried out, the latest one only during the last year (ref. 1). It has there been pointed out that improvement of the collection efficiency in the long wavelength range can contribute an increase of the overall performance of silicon solar cells by as much as 7%. However, it was mentioned that a relatively large thickness of the base region was needed in order to accomplish this. This is somewhat in conflict with recent efforts to decrease the thickness of the solar cells in order to save spacecraft weight. In the same paper, it had also been remarked that a drift field in front of the back contact did not affect the collection efficiency in the thicker cells, but that some observations have been made that indicated that such a drift field might be beneficial in thin cells. In order to fully clarify this point, it was further investigated under this project. This investigation was based on the use of equ. 33 of ref. 2 which permits the calculation of collection efficiency as function of wavelength based on the material and dimension parameters of the solar cell considered. The equation represents the exact solution of the differential equation governing the generation and motion of minority carriers in either the diffused or the base region of the solar cell. The equation is not based on any approximations or on unduly restrictive assumptions. The only general exception to this statement is the condition that current contributions from different wavelengths are linearly superimposed. This means that the spectral response is independent of light intensity or bias light of any wavelength. Expressed in material parameters, this requires that significant trapping effects are not observed, and that the minority carrier lifetime, as well as all other material parameters, are independent of minority carrier concentration in the range of interest. It has been established that these conditions are fulfilled for normal silicon solar cells for light intensities up to several hundred times that of normal, non-concentrated sunlight.

The mentioned differential equation has been solved with the appropriate boundary conditions so as to include two distinct layers in either the base or the diffused region of the solar cell. These two distinct layers can include different material parameters, including impurity density gradients such as to produce a drift field. Equation 33 of ref. 2 constitutes such a solution for a two layer structure in either of the two major solar cell regions. With this feature the equation is uniquely useful for the solution of problems as that at hand.

It may be noted that an explicit solution of the transport differential equation is possible only if the material parameters in each of the sub-regions (or layers) are constant throughout the sub-region. This may not always be the case, particularly if gradients of impurity density exist. Then both minority carrier lifetime and mobility will vary as function of impurity concentration. The solution, however, is based on constant mobility and constant minority carrier lifetime throughout the sub-region. By use of weighted average values for mobility and minority carrier lifetime in the sub-region, calculated collection efficiency values have been obtained which deviate by only a few percent from those obtained by numerical evaluation of the corresponding case with varying material parameters.

2. The Computer Program

The program constitutes a straightforward evaluation of equ. 33 of ref. 2, performing the computation of the collection efficiency as function of wavelength, of the overall collection efficiency weighted by the spectral distribution of the incident light, and of the short circuit current. It had previously been programmed for use on a time-sharing computer system. This program has been transferred to the IBM360-75 computer at the University of Pennsylvania. Although both systems utilize Fortran IV language, the change from a time-sharing system to a card input system necessitated some program changes. The modified program has been debugged and is running well. The input format to the program is shown in Fig. II-1. The first line contains a field for two integer digits as index (subscript) for the beginning of the spectral wavelength range to be used, followed by two integer digits as the index for the end of the wavelength range. The possible wavelength index (subscript) numbers run from 1 through 40, each corresponding to a wavelength interval of 500 Å Angstrom width around a center wavelength starting with 2,000 Angstrom for index "1", and increasing in 500 Å Angstrom steps to 21,500 Å Angstrom for index number "40".

The spectral distribution data for three different light sources are stored in the program: airmass zero sunlight from the wavelength interval centered at 2,000 Å to that centered at 21,000 Å, airmass one sunlight from the wavelength interval at 4,000 Å to that at 11,000 Å, and incandescent light (tungsten filament) at 2,800 °K color temperature from the wavelength interval at 4,000 Å to that at 11,500 Å. Absorption coefficient data at 300 °K and 77 °K are also stored from 2,000 Å to 11,500 Å, and from 4,000 Å to 10,500 Å, respectively. Since each wavelength interval is 500 Å wide, the spectral distribution range for airmass one sunlight, for instance, actually covers the range from 3,750 to 11,250 Å wavelength. The call-out for use of the desired spectral

```
/GO
0119
PHAMO
AB300
0.0         0.0         3.0E-02
0.25E-03
300.0
            1.0E-05     1.25E03
0.0         0.0          0.0        0.0
0.0         0.1E-05     0.4E02      0.0
0.0         0.0         0.0         0.0
0.1E02
0.0         0.0         0.0         0.0         0.0         0.0
0.0         0.0         0.0         0.0
0.0         0.0         0.0         0.0
/END
```

Fig. II-1 Data Input Format for Computer Program SOCEL 2 for the Calculation of Collection Efficiency as Function of Wavelength.

distribution occurs in line 2 by entering either PHAM0 for the airmass zero spectral distribution, PHAM1 for the airmass one spectral distribution, or PHW28 for the 2,800°K tungsten-light spectral distribution. Similarly, in line 3, AB300 calls for the absorption coefficients at 300°K, AB077 for those at 77°K.

Line four contains the entries for the location of region boundaries for the base region, measured from the active surface of the solar cell in cm. Three fields of ten positions each for floating decimal entry are provided. The first field is for entry of the location of the front boundary of the base region (its boundary with the depletion region), the second field for the location of the interface boundary between the two base sub-regions, and the third entry for the interface with the ohmic contact, which is usually identical with the total thickness of the silicon wafer. Line five contains three corresponding entries for the diffused region, in the same format. The sequence here is from the front boundary of the depletion region, to the interface between two different sub-regions in the diffused region, to the front boundary of the diffused region, which is normally zero. Subscripts for the region boundaries are used as follows: the first subscript refers to the major regions of the device, that is, "1" refers to the base region, "2" to the diffused region. The second subscript runs from 1 to 3, "1" referring to the boundary to the depletion region, "2" to the interface boundary between the two adjacent sub-regions, and "3" to the boundary farthest removed from the depletion region. If no entries for interface boundaries are made, the computer will automatically substitute the midpoints between the outside boundaries of the appropriate region. If no entry for the near boundary of the depletion region is made, which is the front boundary of the base region, the front boundary of the depletion region will automatically be

substituted. If the entries between rear boundary and front boundary of the depletion region differ, the computer will consider the depletion as a third region, with a thickness as determined by the difference between the two entries for the depletion region boundaries, and will assume 100% collection efficiency within the depletion region.

The entry in line six is a single number for the temperature of the solar cell, to be entered in fixed decimal point notation with two positions behind the decimal point.

The next four lines contain the entries of the material properties in the four sub-regions of the solar cell for which collection efficiency is to be computed. The arrangement of the subscripts for the regions is as follows: first subscript:"1" refers to the base region, "2" to the diffused region; second subscript: "1" refers to the sub-region adjacent to the depletion region, in either the base or the diffused region, "2" to the sub-region farther removed from the depletion region. There are four entries for each region, to be made in floating decimal notation, with ten positions provided for each, including three positions behind the decimal point. The sequence of the entries is: diffusion length (L) in cm, minority carrier lifetime (τ) in s, minority carrier mobility (μ) in $cm^2V^{-1}s^{-1}$, and diffusion constant (D) in cm^2s^{-1}. If the diffusion constant is entered, but not the mobility, the latter will be determined by the computer. If the diffusion length is not entered, but the minority carrier lifetime, the diffusion length will be computed by the program. Conversely, if the diffusion length is entered, but not the minority carrier lifetime, the latter will be computed. Thus, two entries need to be made here, either mobility or diffusion constant, and minority carrier lifetime or diffusion length. If no entries are made for sub-region 2, the values for sub-region 1 will be automatically entered. This means, that for any region not consisting of two sub-regions, only one set of entries has to be provided.

Line 11 contains two entries, again in floating decimal format with a field of 10 each and three positions after the decimal point. The entries are for the surface recombination velocity at the front (active) surface of the cell, and at the back surface of the cell. If no entry for the surface recombination velocity at the back surface is made, a value of 10^8 cm s^{-1} will be automatically substituted.

Line 12 may contain enteries for the majority carrier concentrations at the boundaries of the respective sub-regions, using first subscripts "1" and "2" for the main regions, and second subscripts "1" through "3" for the boundaries of the sub-regions in the same system as used for the location of the boundaries themselves. Six entries may be made in floating decimal format of ten positions each, with three positions after the decimal point.

Lines 13 and 14, respectively, contain entries for the potential differences that may exist across any one of the four sub-regions, or for the electrostatic field strengths within them. If the electric field is zero in any one of the sub-regions, no entries for the corresponding sub-regions have to be made. Also, only one set of data has to be entered for each respective sub-region; that is, either the carrier concentration at the two boundaries of the sub-region, or the potential difference across or the electric fieldstrength within the subregion suffices. From any of these data sets, the computer will proceed to calculate the electric fieldstrength and enter it into the calculation of collection efficiency.

A typical printout of the results from the computer program is shown in Fig.II-2. This printout is one from the investigation of the diffused region collection efficiency, and the entries of interest in this investigation have been especially marked. The first line contains the subscript numbers of the wavelength intervals used as limits in the calculation, in this case, 1 and 19 corresponding to the wavelength

```
M =  1  NM = 19
PHN(I) = PHAMO(I)
ABCO(I) = AB300(I)
X(1,1) = 0.2000E-04 X(1,2) = 0.1499E-01 X(1,3) = 0.3000E-01
X(2,1) = 0.2000E-04 X(2,2) = 0.1000E-04 X(2,3) = 0.0000E 00
T =  300.00
J    K    CMU(J,K)      D(J,K)       TAU(J,K)     DL(J,K)
1    1    0.125E 04     0.323E 02    0.100E-04    0.180E-01
1    2    0.125E 04     0.323E 02    0.100E-04    0.180E-01
2    1    0.400E 02     0.103E 01    0.300E-06    0.557E-03
2    2    0.400E 02     0.103E 01    0.300E-06    0.557E-03
SRCOMB(1) =  0.100E 09 SRCOMB(2) =  0.400E 05

J    K    V(J,K)        E(J,K)
1    1    0.000E 00     0.000E 00
1    2    0.000E 00     0.000E 00
2    1    0.000E 00     0.000E 00
2    2    0.000E 00     0.000E 00

 I     WL(I)          ECOLLR(2)    ECOLL3       ECOLLR(1)    ECOLL
 1      2000.00      -0.577E 00   0.000E 00    0.466E-14    0.577E 00
 2      2500.00      -0.576E 00   0.000E 00    0.115E-14    0.576E 00
 3      3000.00      -0.577E 00   0.000E 00    0.466E-14    0.577E 00
 4      3500.00      -0.587E 00   0.000E 00    0.102E-07    0.587E 00
 5      4000.00      -0.584E 00   0.000E 00    0.194E 00    0.778E 00
 6      4500.00      -0.318E 00   0.000E 00    0.581E 00    0.900E 00
 7      5000.00      -0.169E 00   0.000E 00    0.778E 00    0.947E 00
 8      5500.00      -0.108E 00   0.000E 00    0.854E 00    0.962E 00
 9      6000.00      -0.741E-01   0.000E 00    0.894E 00    0.968E 00
10      6500.00      -0.541E-01   0.000E 00    0.915E 00    0.969E 00
11      7000.00      -0.395E-01   0.000E 00    0.928E 00    0.967E 00
12      7500.00      -0.294E-01   0.000E 00    0.934E 00    0.963E 00
13      8000.00      -0.185E-01   0.000E 00    0.930E 00    0.948E 00
14      8500.00      -0.124E-01   0.000E 00    0.915E 00    0.927E 00
15      9000.00      -0.762E-02   0.000E 00    0.881E 00    0.889E 00
16      9500.00      -0.358E-02   0.000E 00    0.783E 00    0.786E 00
17     10000.00      -0.141E-02   0.000E 00    0.570E 00    0.571E 00
18     10500.00      -0.515E-03   0.000E 00    0.307E 00    0.307E 00
19     11000.00      -0.156E-03   0.000E 00    0.112E 00    0.112E 00

    ECOLAV =  0.795E 00

SCJR(2) = -0.625E-02   SCJR(1) =  0.393E-01      SCJTOT =  0.455E-01

          PHNRSP = 0.347E 18      COLEFF = 0.821E 00
          PHNTOT = 0.533E 18      CVCOLF = 0.534E 00
```

Fig. II - 2 Computer printout from program SOCEL2. Underlined are parameters which are varied in a particular study.

intervals centered at 2000 and 11,000 Angstroms. The next two lines indicate the spectral distribution and absorption coefficient data used. Subsequently, two lines give the data for the sub-region boundary locations entered into the program for regions 1 (base region) and 2 (diffused region), respectively. Line 6 indicates the operating temperature entered. This is followed by a table for the material constants for the four sub-regions, with subscript J referring to the major region, and K to the sub-region within the major region. The table is followed by a line indicating the surface recombination velocities at the base and the diffused region, in this sequence. The next table contains the values of potential difference and electric field-strength as they apply to each of the four sub-regions. This last table of entry data is followed by a table of computed results. It shows subscript I for the wavelength regions in the first column, the center wavelength of each interval printed out in the second column, followed by the computed collection efficiencies in each wavelength interval for the diffused region, the depletion region, and the base region, in this sequence, in columns 3 to 5. Column 6 finally contains the total collection efficiency of the cell for each wavelength interval as the sum of the collection efficiencies of the three regions. If the depletion region width is entered as zero, the collection efficiency for this region will be zero.

Below the table are additional computed results, including the unweighted average collection efficiency (ECOLAV) obtained from column 6. In the next line, the total light generated current values computed by use of the entered spectral distribution, are shown for the diffused region, the base region, and for the entire cell in this sequence. The next to last line of the printout indicates the total number of photons contained in the spectral distribution curve within the entered wavelength limits (PHNRSP), and the collection efficiency weighted by the spectral distribution (COLLEFF). The last line finally contains the total number of photons in the entire spectral distribution curve contained in the program (PHNTOT), and the overall collection efficiency of the cell, determined from this total spectral distribution curve (OVCOLF).

3. Results of the Computations.

As mentioned above, the preceding work had led to the conclusion that, using a base region with uniform material parameters, high collection efficiency values in the long wavelength part of the spectral response range can be obtained with rather large values of wafer thickness (0.05 cm and above.) Reference 3 indicated, that improvement of minority carrier diffusion length should lead to better collection efficiency in thin silicon solar cells, approaching that of the thicker cells. Since this is in conflict with the expectation that bringing a minority carrier sink, namely the ohmic contact, closer to the depletion region, should not be curable by increasing the diffusion length alone, this point was investigated first. The solid curves of Fig. II-3 summarize the results of this investigation into the effect of diffusion length on collection efficiency from the base region, using wafer thickness as parameter with values of 500 μm (0.020"), 300 μm (0.012"), and 100 μm (0.004"). A base region with uniform material parameters corresponding to 10 Ω cm resistivity and with a normal ohmic contact of high surface recombination velocity (10^8 cm s^{-1}) at the back of the wafer were used.

Total short-circuit current generated in the cell under air mass zero sunlight is plotted in Fig. II-3 as function of diffusion length. However, on the right hand side of the figure, an additional scale has been added for the ordinate to express the data in "collection efficiency."

It is clearly visible in the figure, that increasing the diffusion length has a lesser influence on cells with smaller wafer thickness. In particular, no significant improvement can be expected by increasing the diffusion length beyond the base region thickness, as vividly illustrated by the curve for the 100 μm thick cell. However, introducing a drift field in front of the back contact removes its effect as a minority carrier sink, as shown by the dashed curves of Fig. II-3. Here, the effect of thickness

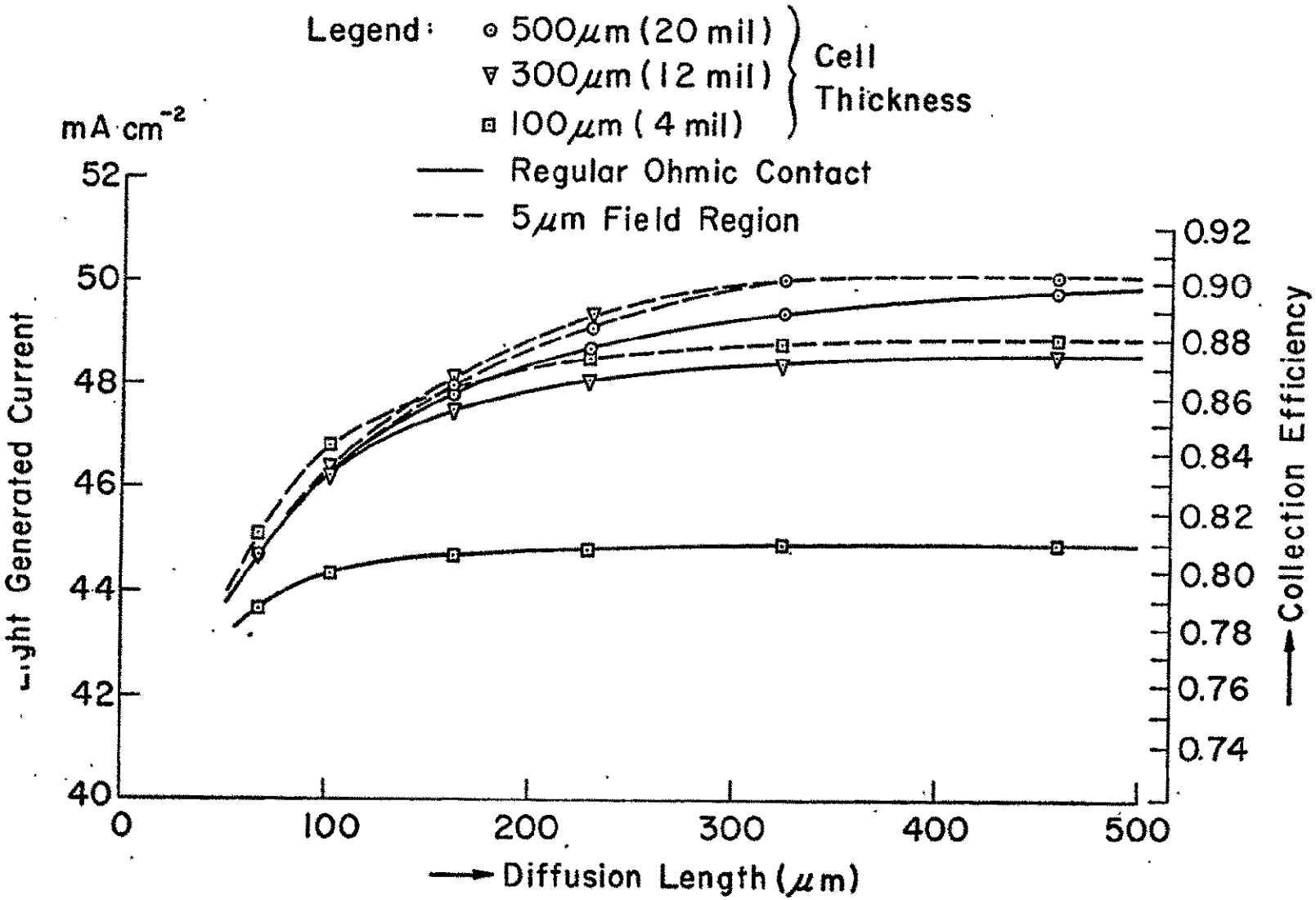

Fig. II – 3 Total shortcircuit current (left ordinate) and collection efficiency η_{coll} (right ordinate) as function of diffusion length for 3 values of thickness for silicon solar cells in airmass zero sunlight.

has largely been eliminated, so that the collection efficiency increases with diffusion length up to values of approximately 3 times the base region thickness. Also, collection efficiency values within a few percent of those of the thick cells are achievable in 100 μm thick cells. The drift field is obtained by introducing a p^+ region into the base region of the cell, just in front of the ohmic contact. The legend in Fig. II-3 is somewhat misleading insofar as it refers to the transition region between the base region and the p^+ region (0.0125 Ω cm) of 5 μm thickness, rather than to the latter being this thick. It may be noted that p^+ regions are occasionally used as silicon solar cells to improve the characteristics of the back contact, rather than to improve collection efficiency in thin cells. Also, there has been evidence, that the diffusion length is degraded in the fabrication of thin cells, and that it can be restored to the values obtained in thick cells by use of gettering processes (ref. 4).

These first calculations on the effects of a drift field were carried out for 5 μm thickness of the field region. Such a large thickness is, however generally not obtained in present cells. The question then arose whether comparable results could be obtained with thinner field regions. In order to eliminate (for the purpose of comparison) the effect of decreased absorption in wafers of lesser thickness, the collection efficiency has been split into two factors:

$$\eta_{coll} = R_{abs} \cdot R_{coll}$$

R_{abs} represents the ratio of the number of photons absorbed in a wafer of thickness d, to the total number of photons incident on the surface of the cell. The second factor, labeled R_{coll}, represents the ratio of the number of minority carriers actually collected at the pn junction to the number generated in this absorption of the photons. Fig. II-4 presents the ratio R_{abs} as function of thickness d for air mass zero

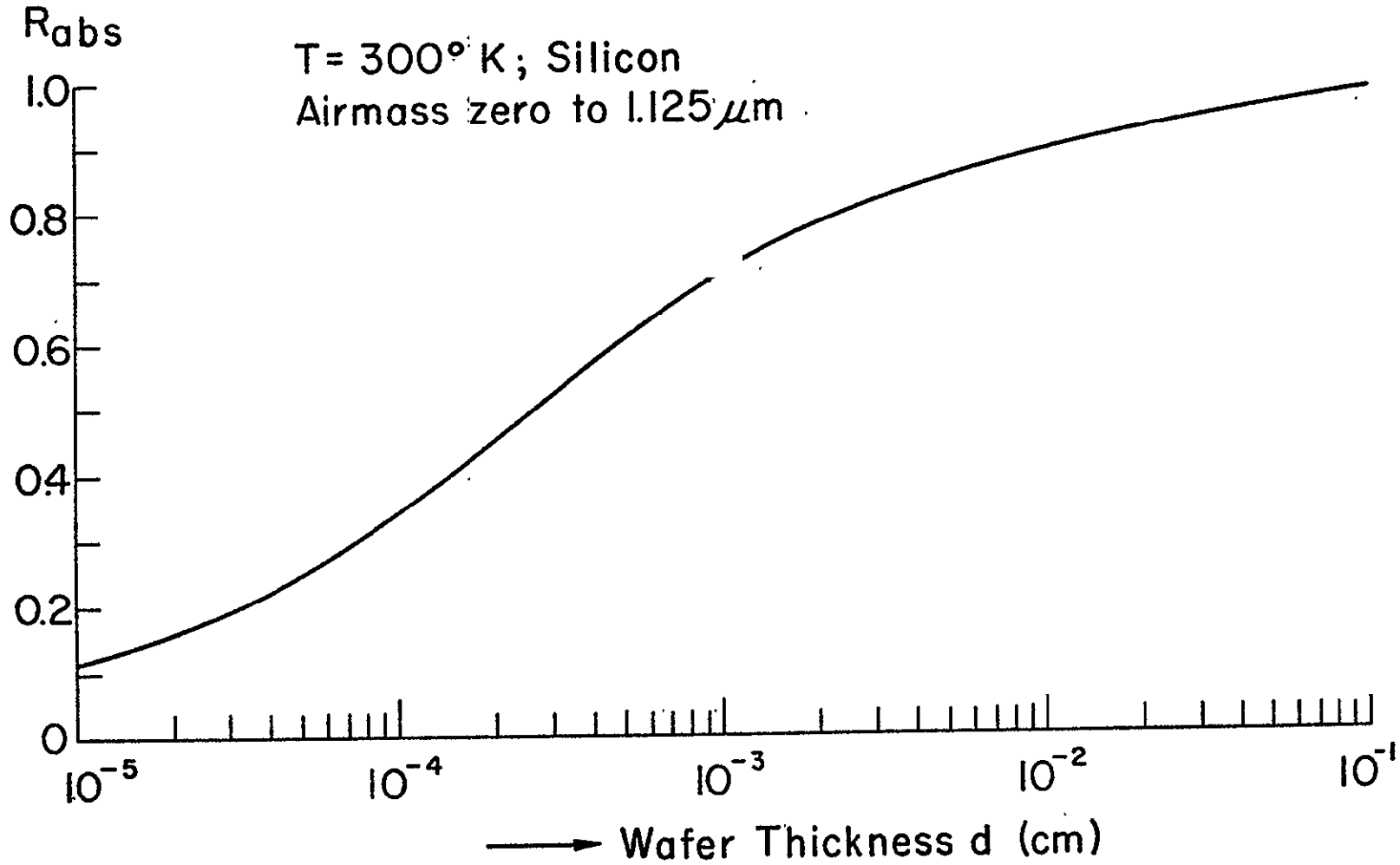

Fig. II - 4 Ratio R_{abs} of the number of photons absorbed in a single pass through a silicon layer of thickness d to the number entering the layer, as contained in airmass zero sunlight up to 1.125 μm wavelength.

sunlight in silicon at 300° K temperature. It should be noted that this ratio refers only to the number of photons contained in the sunlight spectrum up to 1.125 μm wavelength, just as the other collection efficiency data do.

Fig. II-5 then presents the ratio R_{coll} as function of wafer thickness d for cells of 3 different values of diffusion length, with and without a drift field in front of the back contact. It is again evident that the drift field has no influence at large values of wafer thickness. The reason is that the back contact as well as the drift field are removed from the depletion region by substantially more than a diffusion length, so that their properties can not significantly affect the collection efficiency. On the other hand, it is clearly visible that the diffusion length substantially influences the overall collection efficiency by increasing the "effectve wafer thickness", as compared to the "physical wafer thickness" entering into R_{abs}. The fact that R_{coll} increases with decreasing wafer thickness towards medium wafer thickness for the smaller values of diffusion length may appear puzzling at first, but is readily explainable as follows: A number of photons is absorbed well beyond the diffusion length in thick wafers, which would not be absorbed in the wafer of smaller thickness. This results in smaller values of $\overline{R_{abs}}$ for the thinner wafers. The minority carriers potentially generated from these photons would not be collected in either a thick or a thin wafer, resulting in approximately equal values of the collection efficiency η_{coll} (see Fig. 1, 300 and 500 μm thickness). Since, in a thin wafer, the effect of these photons enters into R_{abs}, this permits R_{coll} to appear more favorable.

The interesting aspect of Fig. II-5, however, is again the fact that with a drift field (in this case 0.1 μm thick) in front of the back contact, substantially higher values of R_{coll} are obtained than without the field at the smaller wafer thickness. To emphasize again, the collection efficiency at the small wafer thickness is not greater than that of a thick wafer, since the good value of R_{coll} is multiplied by a considerably lower value of R_{abs}.

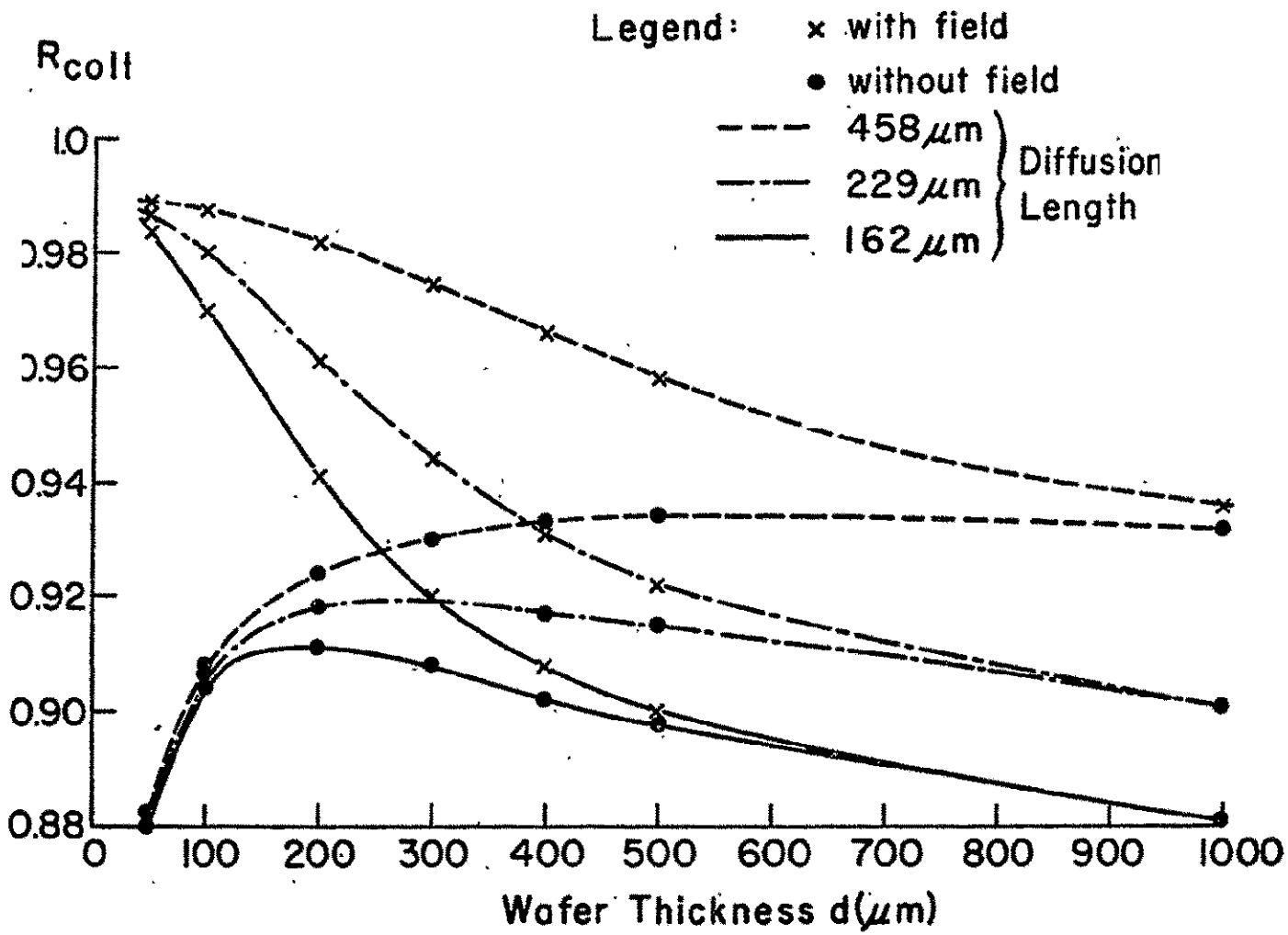

Fig. II - 5 Ratio R_{coll} of the number of minority carriers collected to the number of photons absorbed in a silicon solar cell of thickness d, for 3 values of diffusion length in the base region, with and without a drift field in front of the back contact. Airmass zero sunlight, T = 300° K.

Finally, the effects of the thickness of the drift field layer in front of the back contact and of the median diffusion length within this field layer were investigated. The more illustrative of the data obtained are summarized in Fig. II-6, showing R_{coll} as function of drift field layer thickness. The calculations represented in this figure were carried out for cells of 100 μm thickness, a thickness which is practical, and where the drift field has a significant influence. Here, the interesting observation can be made that at values of drift field layer thickness as low as 0.1 μm, practically the same value of R_{coll} can be obtained as with layer thicknesses as high as 5 μm. However, the diffusion length in a thinner drift field region can be smaller than that required for optimization in a thicker drift field region. It has thus been shown that even with very thin drift field regions, a large improvement in collection efficiency can be obtained in thin solar cells.

4. Conclusions

1. Thin silicon solar cells can be prepared with nearly the same collection efficiency as thick cells, the difference being determined essentially only by the smaller number of photons absorbed, as expressed by R_{abs}. (Fig. II-4).
2. p^+ regions, as occasionally introduced for the improvement of the ohmic back contact, will provide this collection efficiency improvement in thin cells.
3. The thickness of the field region and of the p^+ region is not critical. A field region thickness of 0.03 μm is definitely sufficient.
4. A diffusion length value of approximately 300 µm is sufficient to approach maximum collection efficiency in both thick and thin sola cells.
5. Decreased wafer thickness will also affect the current voltage characteristic (detrimentally!). The drift field cannot be expected to be equally beneficial here. This ar-
the subsequent parts of this study.

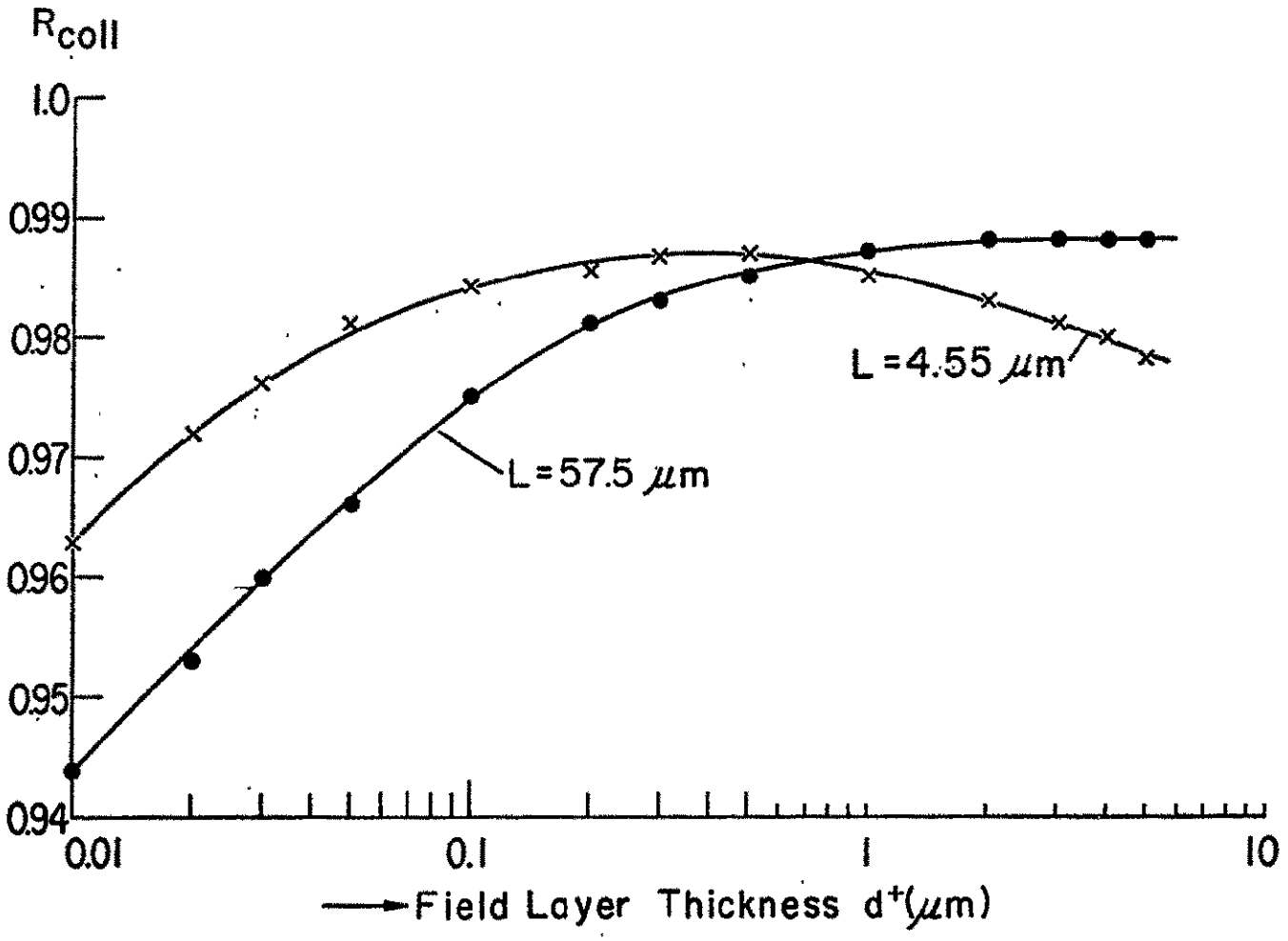

Fig. II - 6 Ratio R_{coll} as function of thickness of the drift field layer in front of the back contact for 2 values of median diffusion length in the drift field layer, for an impurity concentration ratio of 10^4 between p^+ region and base region.

5. References to Section II

Ref. 1

M. Wolf, "A New Look at Silicon Solar Cell Performance", Conference Proceedings of the 8th Photovoltaic Specialists Conference, pp. 360 -371, Aug. 4 - 6, 1970, Seattle, Wash. To be published in Energy Conversion, Pergamon Press.

Ref. 2

M. Wolf and E.L.Ralph, "Effect of Thickness on Short Circuit Current", Conference Record of the 4th Photovoltaic Specialists Conference, June 2, 1964, Cleveland, Ohio.

Ref. 3

R. Gereth, H. Fischer, E. Link, S. Mattes, and W. Pschunder, "Silicon Solar Cell Technology of the Seventies", Conference Record of the 8th IEEE Photovoltaic Specialists Conference, pp. 353 - 359, Aug. 4 - 6, 1970, Seattle, Wash.

Ref. 4

R. Gereth, H. Fischer, private communication

III. The Influence of Material and Design Parameters on the Collection Efficiency in the Diffused Region

1. Introduction

In past development efforts on silicon solar cells, the performance of the diffused region has been improved primarily through work on two parameters only: on the thickness of the diffused region, and on optimization of the anti-reflection coating. Since the diffused region contributes to the collection of minority carriers primarily in the short wavelength region, where photons have a small penetration depth, the results of these efforts towards performance improvement have been connected with names like "blue solar cell" and "super blue solar cell."

The most recent investigation into potential performance improvement of silicon solar cells (ref. 1) has led to the conclusion that the collection of minority carriers which are generated by the absorption of short wavelength photons, can be considerably improved through a reduction of the surface recombination velocity combined with a further reduction of the thickness of the diffused region. This improvement is achievable while maintaining the minority carrier lifetime at the presently observed value near 3 ns. In a later section of the same paper, however, it was observed that, in the interest of obtaining high open circuit voltages and curve factors, attainment of a minority carrier lifetime in the diffused region of 4μs would be desirable. It is clearly of interest that these two differing statements, both relating to performance improvement of silicon solar cells, be tied together. Beyond this, it is very worthwhile to investigate the interrelation of the various material and design parameters of the diffused region in their influence on the collection efficiency from this region. Such an investigation should provide answers to questions such as: What minority carrier lifetime, or diffusion length, will be necessary for high performance from a given thickness of diffused region? How thick or thin

should the diffused region really be for optimum performance? How low a value of surface recombination velocity should one strive for? , and so forth.

To obtain the answers to such questions, a comprehensive theoretical investigation of the influence of material and design parameters on the performance of the diffused region was undertaken, and its results are described and discussed in this section. The investigation was carried out through use of the same theoretical relationship and computer program described in the preceding section. The important parameters varied in this study, are the surface recombination velocity at the exposed surface of the diffused region, the minority carrier lifetime in the diffused region, and the thickness of this region as given by the distance between the exposed surface and the edge of the depletion region of the pn junction. The computations yield the collection efficiency as function of wavelength, separately for the diffused region and the base region of the solar cell, as well as combined for the entire cell, the light generated current contributions from the two regions and from the entire cell, as produced by airmass zero sunlight, and the overall collection efficiency, weighted by the spectral distribution of this sunlight up to 1.125 μm wavelength.

Of the two physical parameters mentioned, the anti-reflection coating is essentially a device external to the solar cell, which does not directly interact with the material or physical device parameters considered in the following discussions. In these discussions, therefore, the anti-reflection coating will be omitted and the assumption made that the solar cell will be a black absorber, as if an ideal anti-reflection coating had been applied. Such a solar cell is a device with 100% absorption at all wavelengths in the range of interest, i.e. for a silicon cell from approximately 0.3 to 1.125μm. It is clear that, for the ultimate performance evaluation, an allowance has to be made for the difference between such an ideal anti-reflection coating and the performance of real, achievable ones.

2. Results of the Computations

The calculated collection efficiency curve for a diffused region of 0.4μm thickness, having a minority carrier lifetime of 3 ns and a surface recombination velocity of 10^5 cm s^{-1} is shown in Fig. III-1. These are the values which apply to typical, present day silicon solar cells of 10 Ωcm base resistivity, and which have been found to yield a theoretical spectral response curve closely matching those obtained experimentally (ref.2). It is very evident in this figure that the collection efficiency drops off radically below 0.5μm wavelength where a significant amount of solar energy falls on the active surface of the solar cell, particularly with the airmass zero spectrum. As was recognized in the recent publication by this author (ref. 1), improvement of collection efficiency in this wavelength range would not only be desirable, but also most likely achievable.

Fig. III-2 presents the collection efficiency as function of wavelength for a solar cell of same junction depth (0.4μm), but with a considerably improved hole lifetime (300 ns) in the diffused n-type region. Surface recombination velocity has been used as a parameter in this figure, resulting in collection efficiencies varying from approximately 0.08 to 0.87 at 0.3μm wavelength. The curves shown represent the contribution from the diffused region and the total collection efficiency from the entire cell. As expected, the long wavelength portion of the collection efficiency for the entire cell is not influenced by changes in surface recombination velocity on the diffused region. It may be noted that the parameters used for the base region of the cell correspond to those of a good, present-day 0.3 mm (0.012") thick "n on p" silicon solar cell.

Two items appear noteworthy in examining Figure III-2: First, most of the change in short wavelength collection efficiency is caused by a change in surface recombination velocity by one order of magnitude only; and, second, the overall collection efficiency for the entire cell, weighted by the airmass zero sunlight spectrum up to 1.125μm wavelength, is 0.847 for the surface recombination velocity of 4×10^3 cm/sec, while that for the cell with a surface

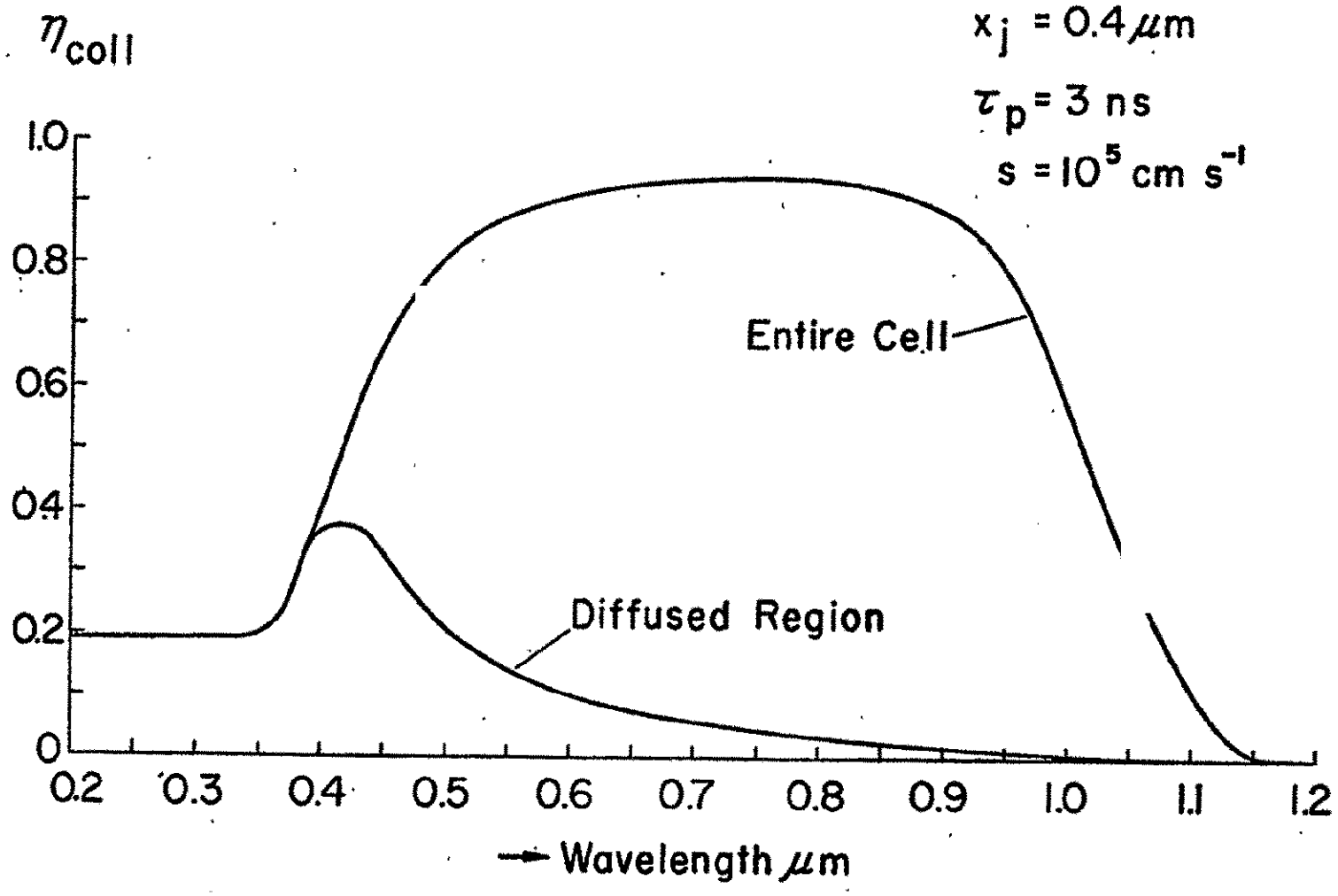

Fig. III-1 Collection efficiency η_{coll} versus wavelength curve for a diffused region corresponding to present, commercial silicon solar cells (ref. 1).

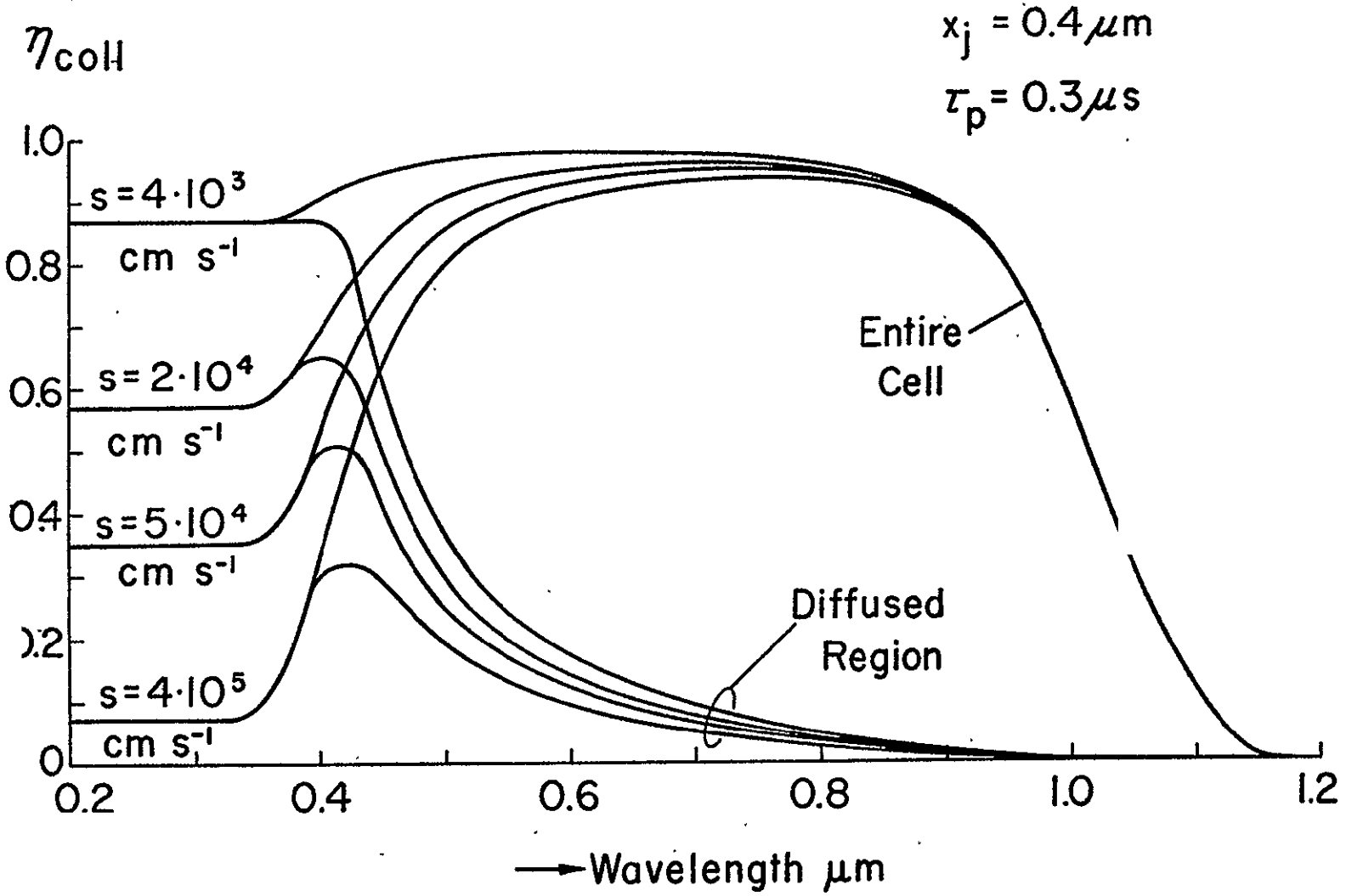

Fig. III-2 Collection efficiency as a function of wavelength from a diffused region of thickness $x_j = 0.4\,\mu m$ with a minority carrier lifetime τ_p of $0.3\,\mu s$, for several values of surface recombination velocity s.

recombination velocity of 4×10^5 cm/sec is 0.7. This means that the overall collection efficiency of the entire cell is only moderately affected by changes of the collection efficiency at very short wavelengths, even if these changes amount to an order of magnitude or more.

Fig. III-3 shows a similar set of curves for the same thickness of the diffused region. Here, however, the surface recombination velocity is constant and 100 cm s^{-1}, and the hole lifetime is used as parameter. The collection efficiency at 0.3 μm wavelength, and the overall collection efficiency under the airmass zero sunlight spectrum vary over approximately the same ranges as in Fig. III-2, and again the entire collection efficiency change is caused by a change in minority carrier lifetime of essentially one order of magnitude only.

In comparing Figs. III-3 and III-2, a few interesting observations are made: first, the general shapes of the collection efficiency curves (that is, the spectral response from a constant number of photons), are rather similar to each other for widely varying values of minority carrier lifetime and surface recombination velocity. This is deduced from the bottom curves of both figures, for which the minority carrier lifetime is 0.15 ns in one case and 300 ns in the other, while the surface recombination velocities are 100 cm s^{-1}, and 4×10^5 cm s^{-1}, respectively. One might thus superficially conclude that the same effect can be obtained with changes in either one of two different material parameters. Second, in the wavelength range between 0.4 and 0.45μm, a diffused region with a longer minority carrier lifetime exhibits a larger collection efficiency than one with a shorter lifetime. This effect was expected, since the absorption coefficient in silicon increases towards shorter wavelengths, reaching its largest values at wavelengths below 0.4μm. Thus, the minority carriers resulting from the absorption of photons will be concentrated most closely to the surface for photons of wavelength below 0.4μm, with the result, that

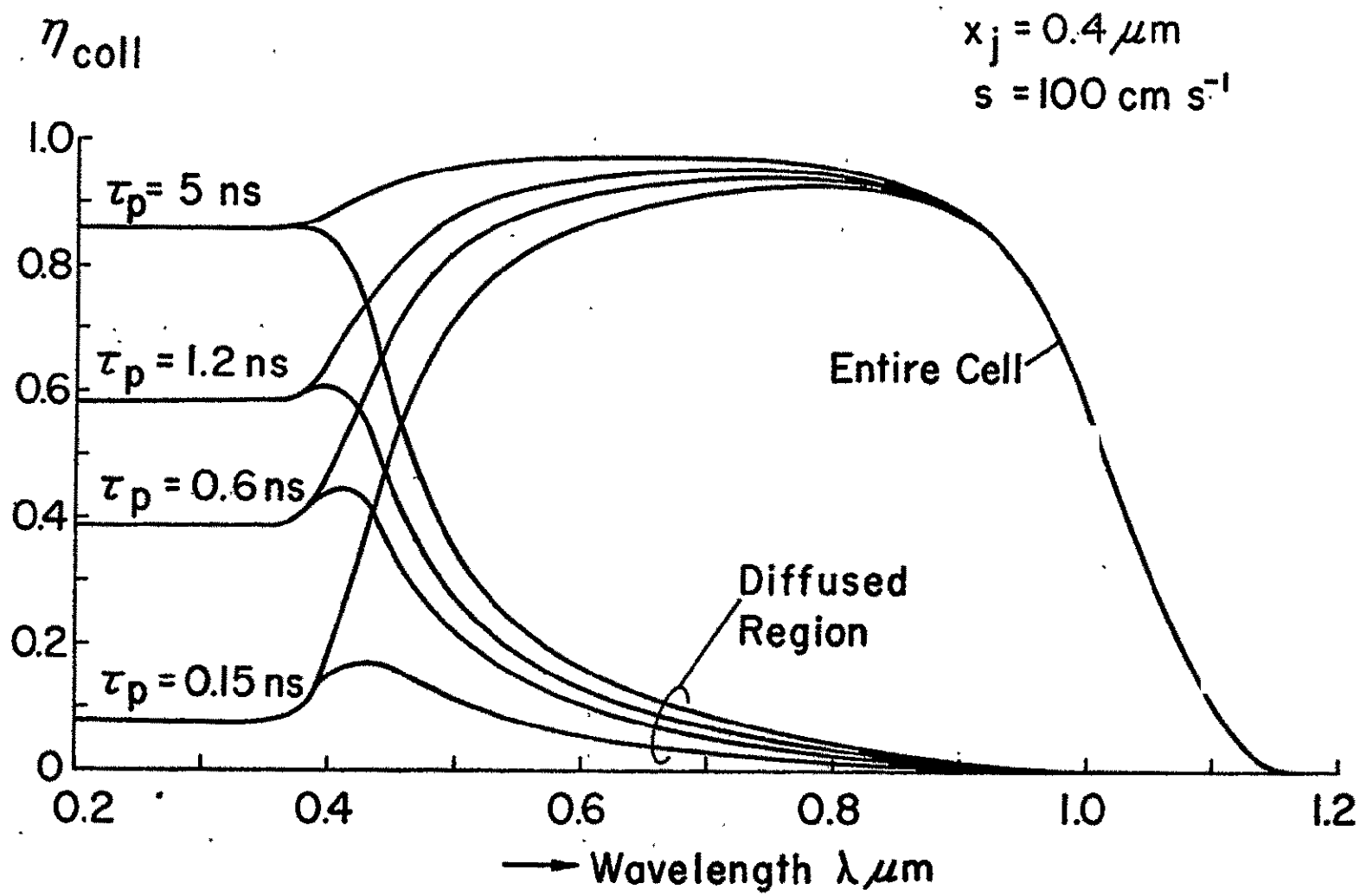

Fig. III-3 Collection efficiency as function of wavelength for several values of minority carrier lifetime τ_p, with surface recombination velocity $s = 100\ cm\ s^{-1}$.

the surface recombination velocity will have its greatest effect at these wavelengths. On the other hand, minority carriers generated from photons penetrating slightly deeper will be more affected by minority carrier lifetime than by surface recombination velocity. Thus, the photons in the 0.4 to 0.45μm wavelength range should be more effectively collected in cells with better minority carrier lifetimes, as is confirmed in Fig. III-2 and III-3.

The question arises, however, whether the effect will be large enough to permit determination, from experimentally obtained spectral response curves, which of the two parameters--minority carrier lifetime or surface recombination velocity--needs modification in order to achieve a collection efficiency improvement. Figues III-4 and III-5 show, therefore, the collection efficiency and the spectral response curves, respectively, for two cells having the same collection efficiency at 0.3μm wavelength, with o having a minority carrier lifetime of 0.3μs. and a surface recombination velocity of 4×10^5 cm s^{-1}, while the other has a minority carrier lifetime of 0.15 ns and a surface recombination velocity of 100 cm s^{-1}. Fig. III-4, the collection efficiency curve, shows a rather large difference between the two types of cell in the short to medium wavelength range. However, the spectral response curves, taken with constant light intensity rather than constant number of photons, represent the normally performed type of measurement. In this mode of measurement, the response in the short wavelength region is depressed, and the sensitivity for observation of material parameter changes in the diffused region thus reduced. Inspection of Fig. III-5 shows that the differences between the two curves are still significant, amounting to as much as 100% of the measured values at some wavelength values. For the adequate analysis of the material parameters in the diffused region, however, it will be necessary to perform very precise spectral response measurements down to at least 0.3μm wavelength. To accomplish such precision, the use of the common, relatively low color-temperature incandescent light sources in the monochromator can be ruled out. Rather, use of a UV monochromator with a light source with high

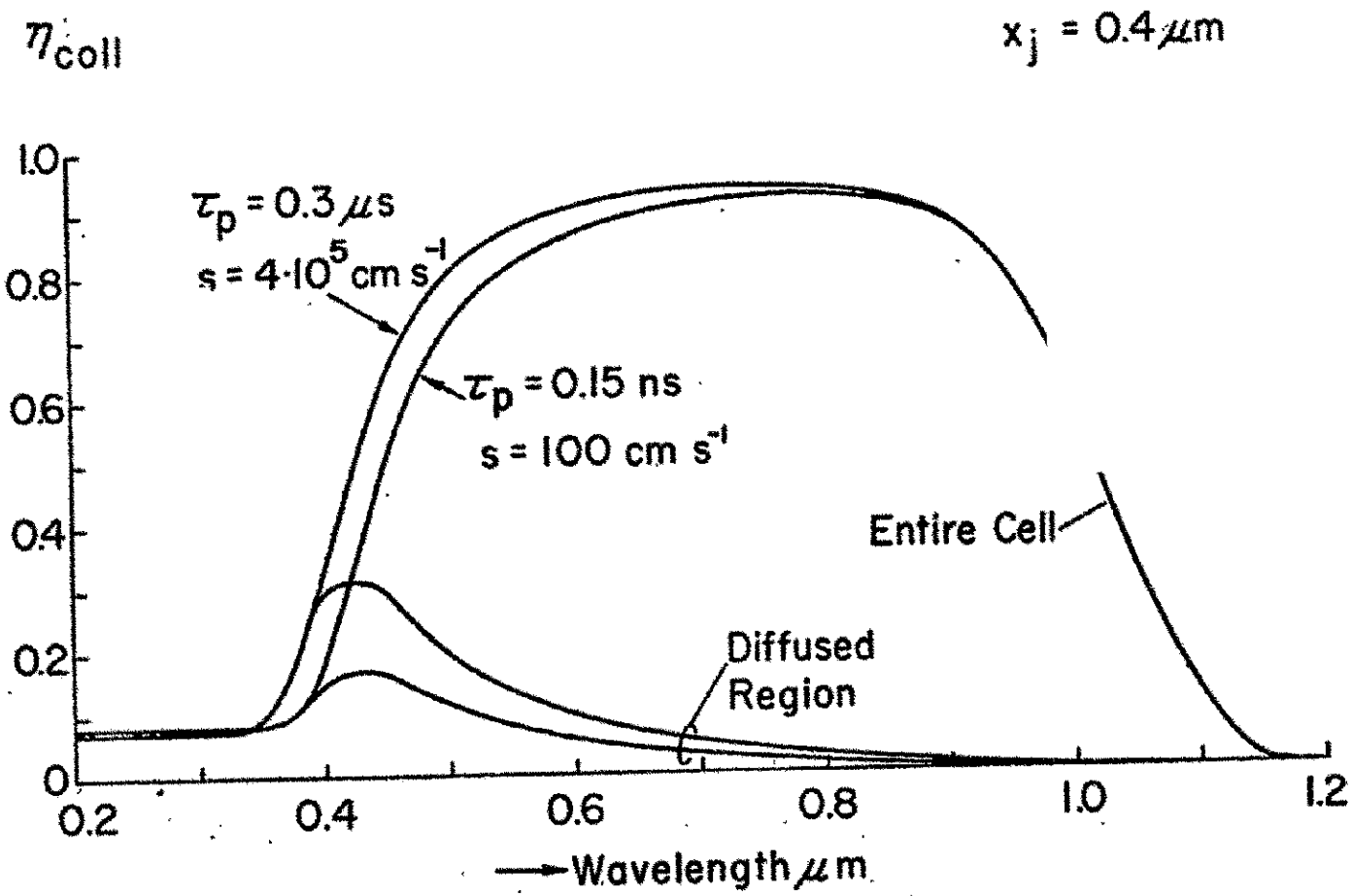

Fig. III-4 Two collection efficiency curves with nearly equal collection efficiency near 0.3 η m wavelength, obtained with different diffused region material constants.

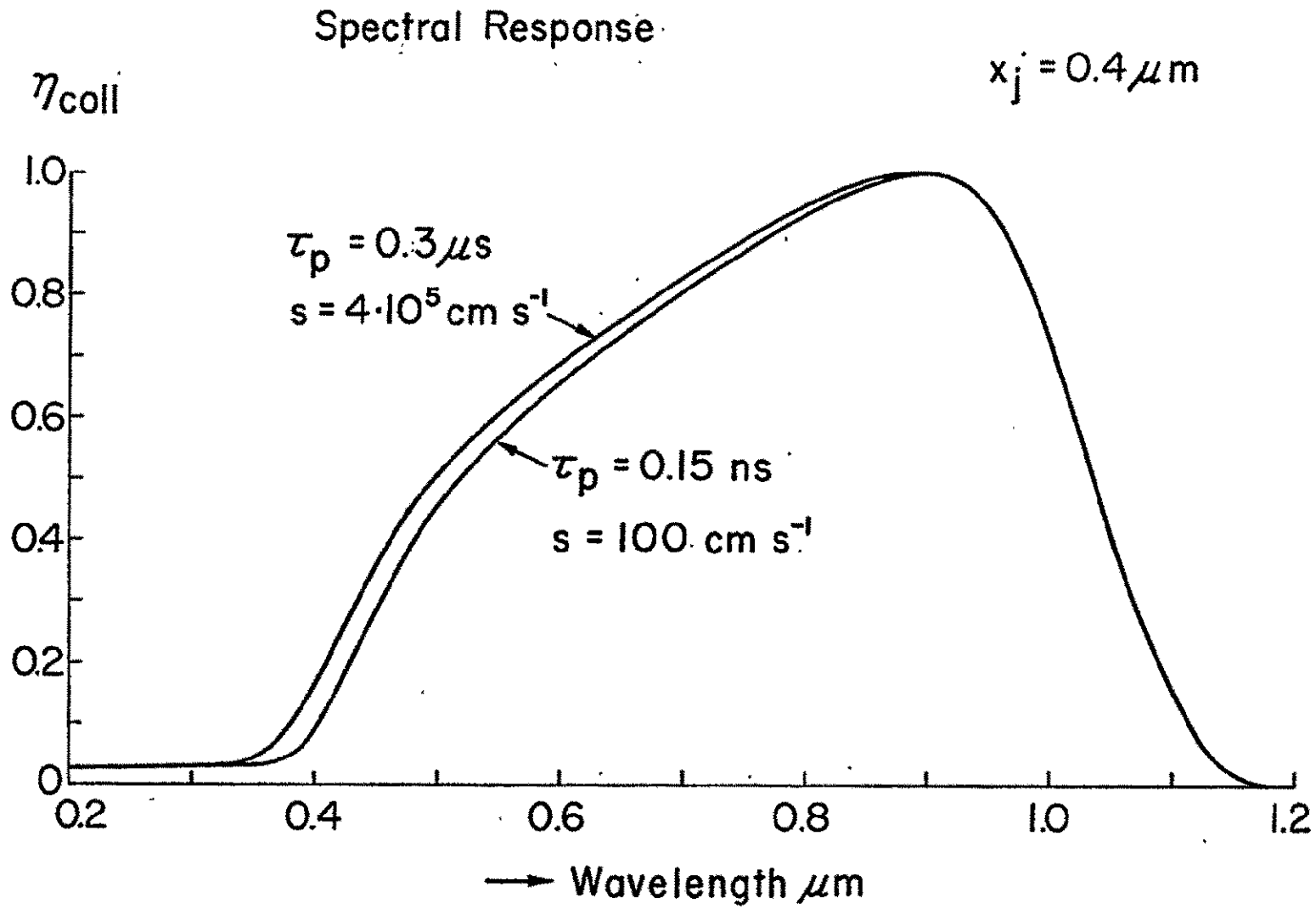

Fig. III-5 Spectral response curves corresponding to Fig. III-4.

intensity in the UV and short wavelength visible regions will be a necessity for work on the improvement of the short wavelength response of silicon solar cells.

Figures III-2 and III-3 led to the conclusion that a different presentation of the data would be desirable to better display the dependence of diffused region performance on the material parameters. Therefore, Fig. III-6 shows the light generated current contribution from the diffused region under the air mass zero sunlight spectrum plotted as function of minority carrier lifetime for five different values of surface recombination velocity. These five values cover four orders of magnitude, although most of the transition is accomplished within one order of magnitude. The figure indicates also that the transition from low values of light generated current to high values is accomplished within two orders of magnitude in minority carrier lifetime. This transition region appears to be essentially independent of the value of surface recombination velocity.

It is also evident from Fig. III-6 that the material parameters of the present cell, namely 3 ns minority carrier lifetime and 10^5 cm s^{-1} surface recombination velocity, are rather unsuitably chosen for achievement of good collection efficiency from the diffused region. As a matter of fact, the minority carrier lifetime is so low as to fall into the transition region. However, in view of the high surface recombination velocity, an improvement in minority carrier lifetime alone would bring no significant results. In order to obtain a high light generated current contribution from the diffused region, the minority carrier lifetime will have to be increased by about one order of magnitude, simultaneously with the improvement in surface recombination velocity. On the other hand, as was suggested ref. 1, the minority carrier lifetime improvement might be circumvented by a decrease in the thickness of the diffused region.

Fig. III-7 contains a similar set of curves for the diffused region of 0.4 μm thickness, in this case, however, presenting the light generated current contribution as function of surface recombination velocity, with minority

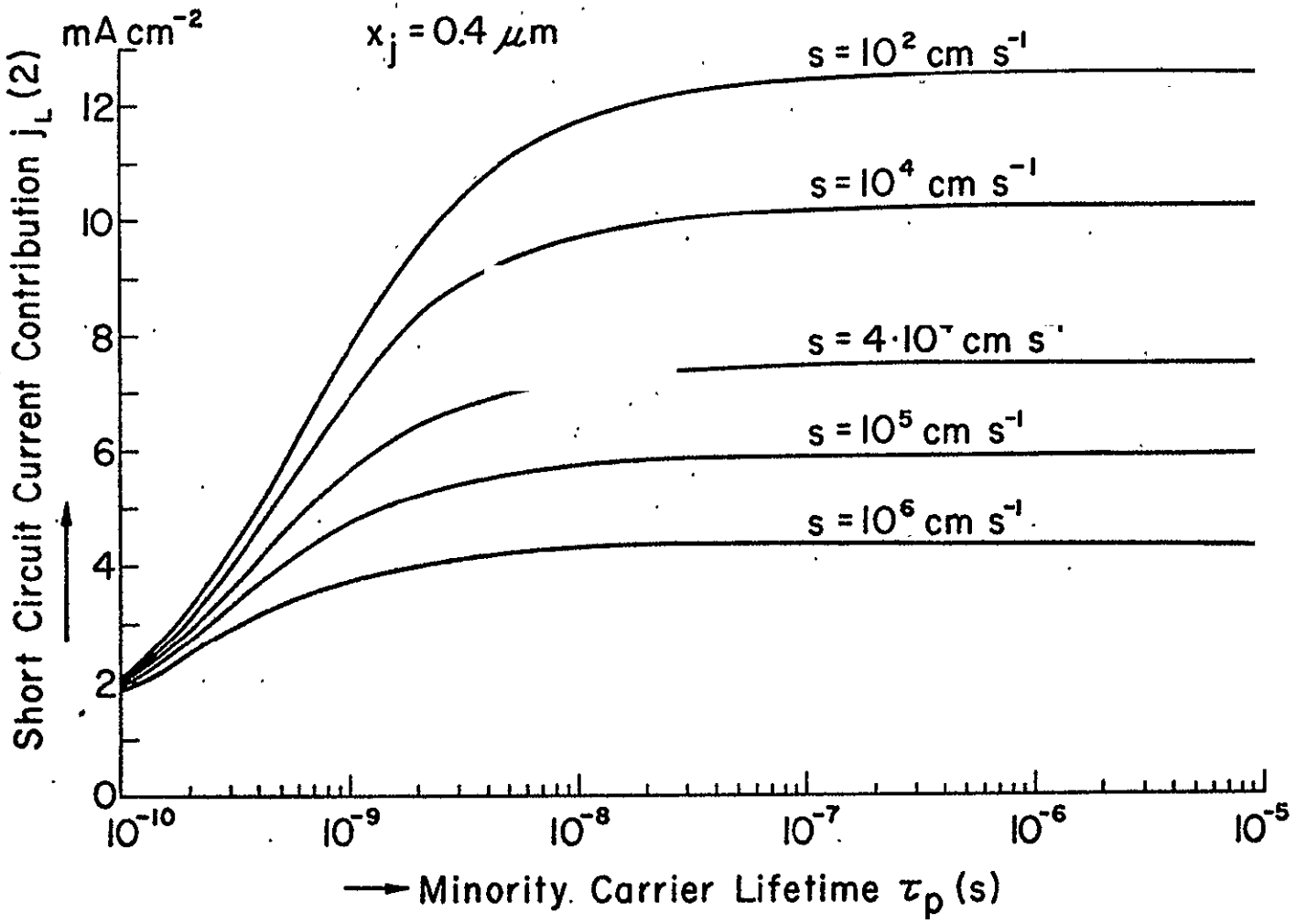

Fig. III-6 . Short circuit current contribution from the diffused region as function of minority carrier lifetime, for several values of surface recombination velocity s. (Diffused region thickness $x_j = 0.4\ \mu m$).

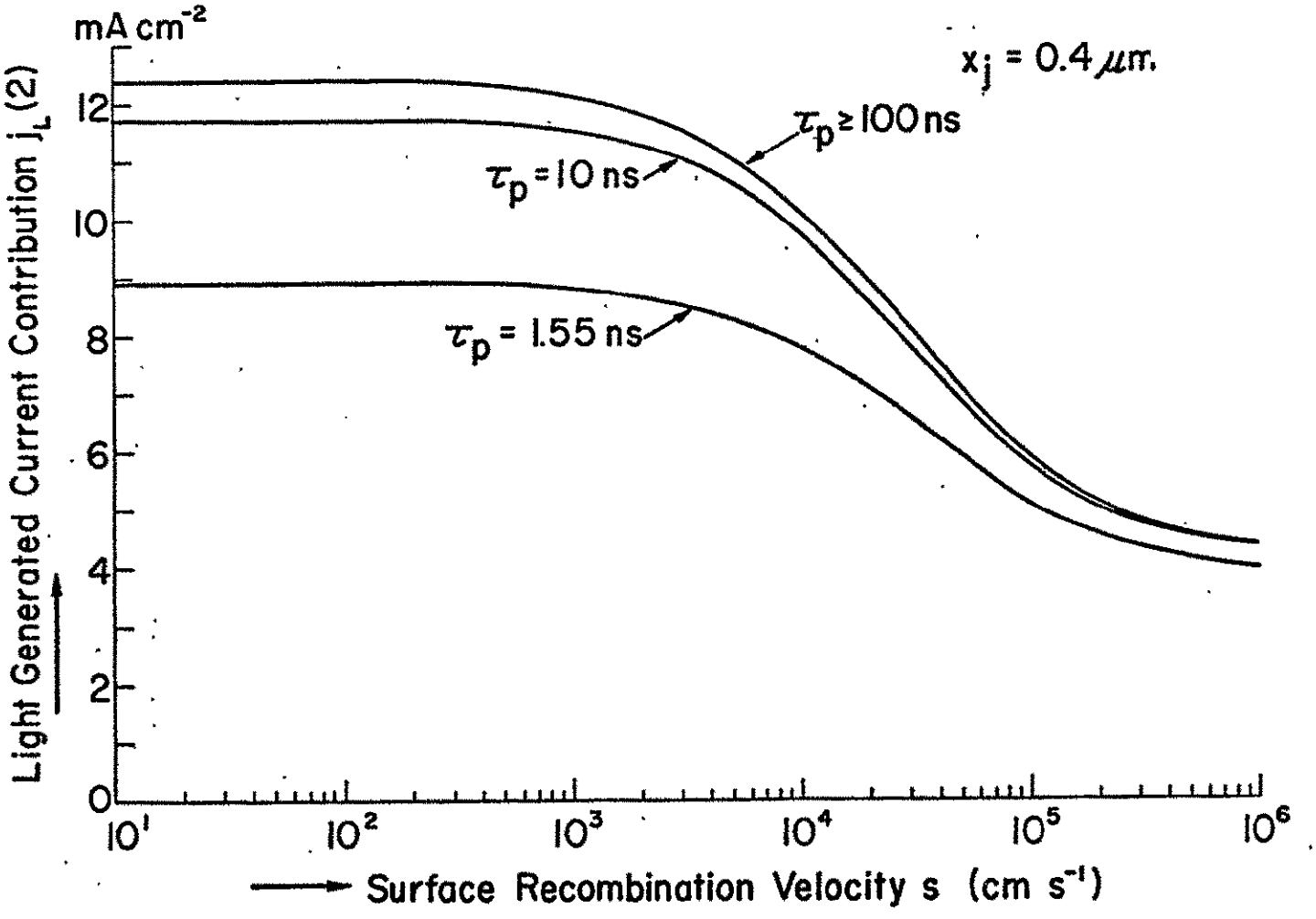

Fig. III-7 Short circuit current contribution from the diffused region as function of surface recombination velocity, for several values of minority carrier lifetime τ_p.

carrier lifetime as parameter. As was seen to be the case in Fig. III-6, the curves are S-shaped, with a transition region in surface recombination velocity containing values within approximately two orders of magnitude. In order to obtain maximum light generated current contributions from the diffused region, surface recombination velocities of 10^3 cm s^{-1} are fully satisfactory, as Fig. III-7 indicates. Values as low as 100 cm s^{-1}, as given in ref. 1, would not bring any significant advantage.

After the effects of minority carrier lifetime and surface recombination velocity have been thoroughly investigated in the previous paragraphs for a fixed value of the thickness of the diffused region, it was thought to be of considerable interest to extend the investigation to the influence of the junction depth. In the previous publication (ref. 1), use of a diffused region thickness of 0.2μm had been suggested. This thickness will therefore be investigated next. However, once higher values of minority carrier lifetime and lower surface recombination velocities can be obtained, it may not be impossible to utilize diffused regions of greater thickness. Therefore, the further discussion will also be extended to greater values of x_j.

Figure III-8 shows a plot of collection efficiency versus wavelength for a 0.2μm thick diffused region, having a minority carrier lifetime of 0.3μs, with surface recombination velocity used as parameter. The graph is similar to Fig. III-2. However, it may be observed that the small peak in the collection efficiency contribution from the diffused region alone has moved to somewhat shorter wavelengths, and that it falls off more rapidly towards longer wavelengths in comparison to the thicker diffused region. It will also be noted that slightly larger values of surface recombination velocity appear to yield similar collection efficiency values in the thinner diffused region, compared to those computed for the greater junction depth.

Fig. III-9 presents the corresponding set of curves for a constant surface recombination velocity of 100 cm/s, with minority carrier lifetime used as the parameter. The prime purpose of this figure is to permit comparison with the corresponding Fig. III-3 for the diffused region thickness of 0.4μm. Beyond this, all observations to be made from these curves have already been

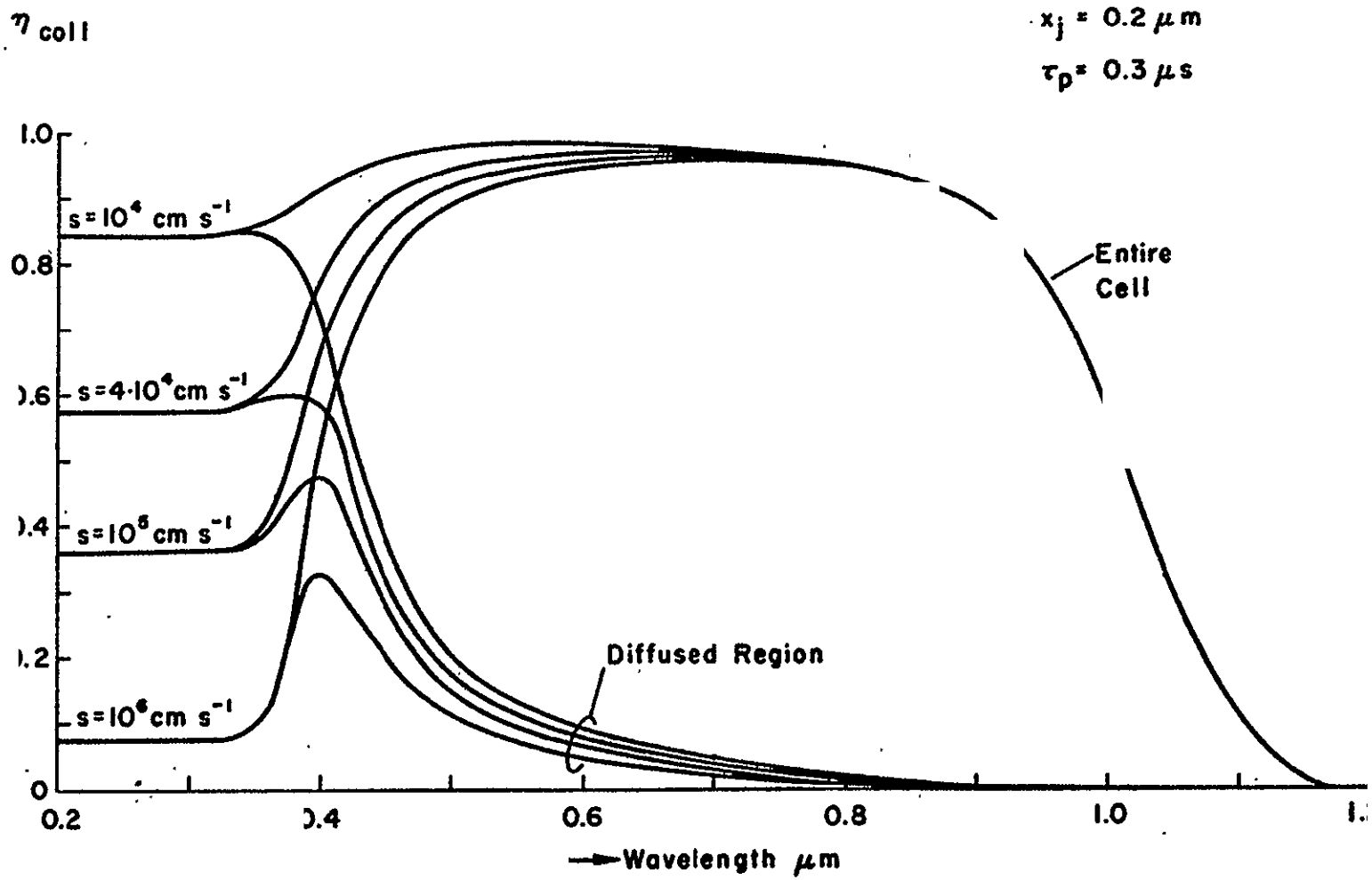

Fig. III-8 Collection efficiency as a function of wavelength from a diffused region of thickness $x_j = 0.2\,\mu m$ with a minority carrier lifetime τ_p of $0.3\,\mu s$, for several values of surface recombination velocity s.

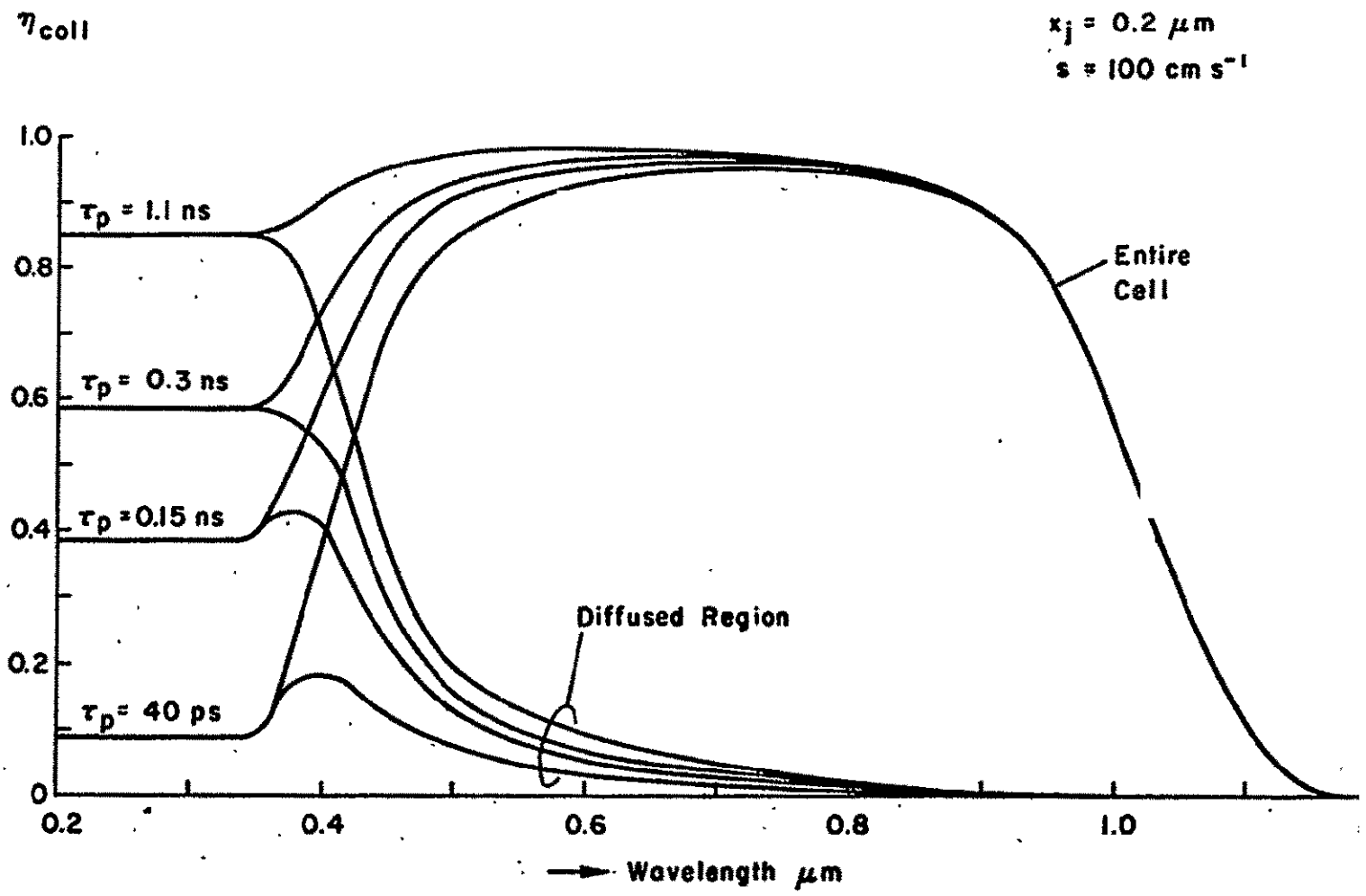

Fig. III-9 Collection efficiency as function of wavelength for several values of minority carrier lifetime τ_p, with surface recombination velocity s = 100 cm s^{-1}.

discussed. Again it was felt to be desirable to display the dependence of the light generated current on the material parameters more directly. Thus, Fig. III-10 presents a plot of the light generated current contribution from the diffused region as function of minority carrier lifetime, with surface recombination velocity as parameter. Fig. III-10 is similar to Fig. III-6, except that it applies to a junction depth of 0.2 μm. The only difference noted in the comparison of these two figures is the shift of the transition region in minority carrier lifetime to lower values. The magnitude of this shift is approximately a factor of four, as would be expected from the relationship between diffusion length and minority carrier lifetime, if the ratio between diffusion length and diffused region thickness is kept constant in order to maintain equal performance.

Fig. III-11 shows the corresponding set of curves for the current contribution from the diffused region as function of surface recombination velocity, with minority carrier lifetime as parameter. Again, a general similarity to Fig. III-7 is noted with the previously made observation that the transition region in the surface recombination velocity is shifted slightly towards larger values of this quantity. Two additional observations may be made here. A minority carrier lifetime of 3×10^{-10} s corresponds to a diffusion length, the magnitude of which equals 0.88 times the thickness of the diffused region. In the past it has generally been considered to be a requirement for good diffused region performance, to have its diffusion length equal the thickness. Fig. III-11 shows clearly that this requirement results in performance of the diffused region which is far from ideal. Rather, a diffusion length greater than three times the diffused region thiskness is required in order to approach the ideal performance of the diffused region.

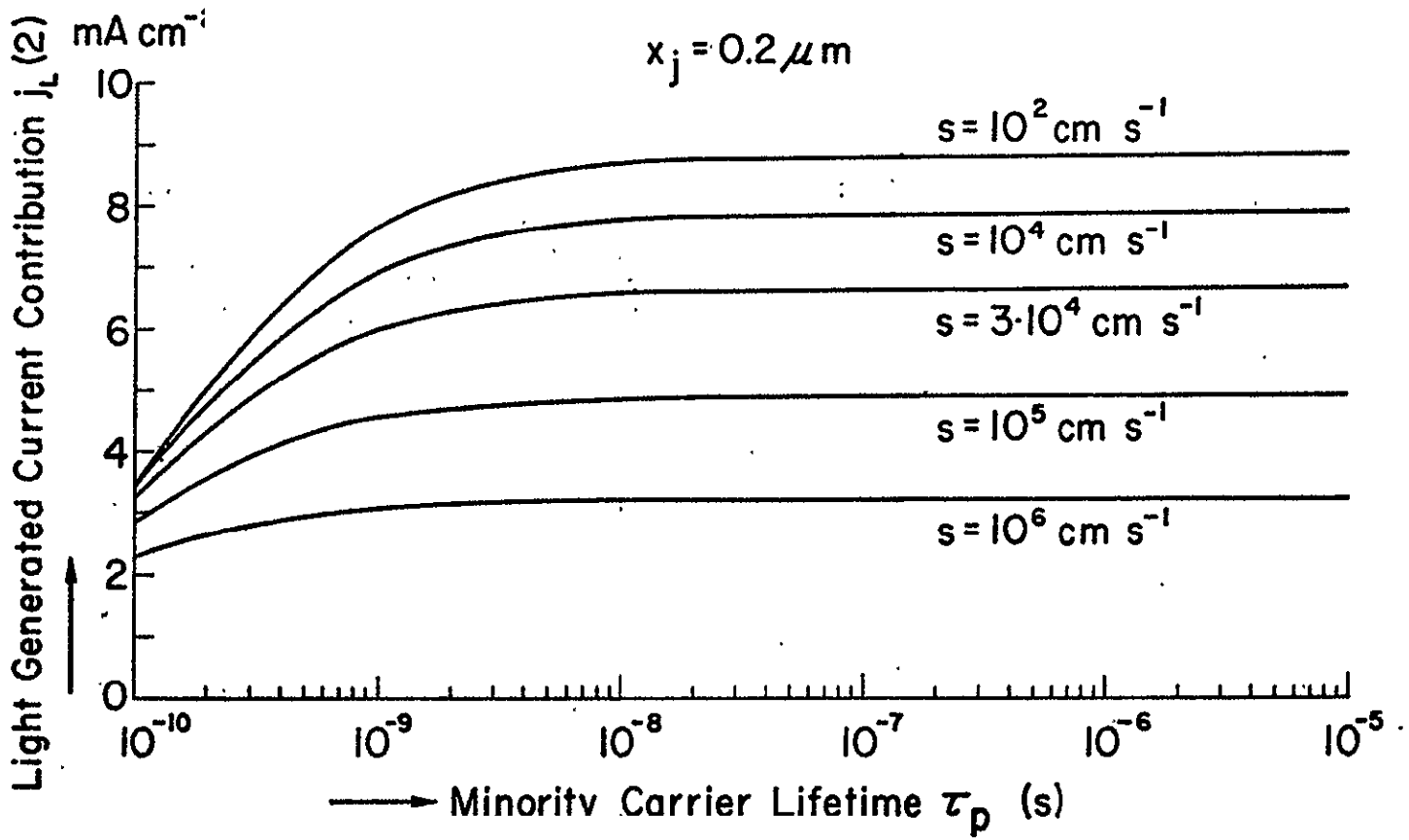

Fig. III-10 Short circuit current contribution from the diffused region as function of minority carrier lifetime, for several values of surface recombination velocity s. (Diffused region thickness $x_j = 0.2_\mu$ cm)

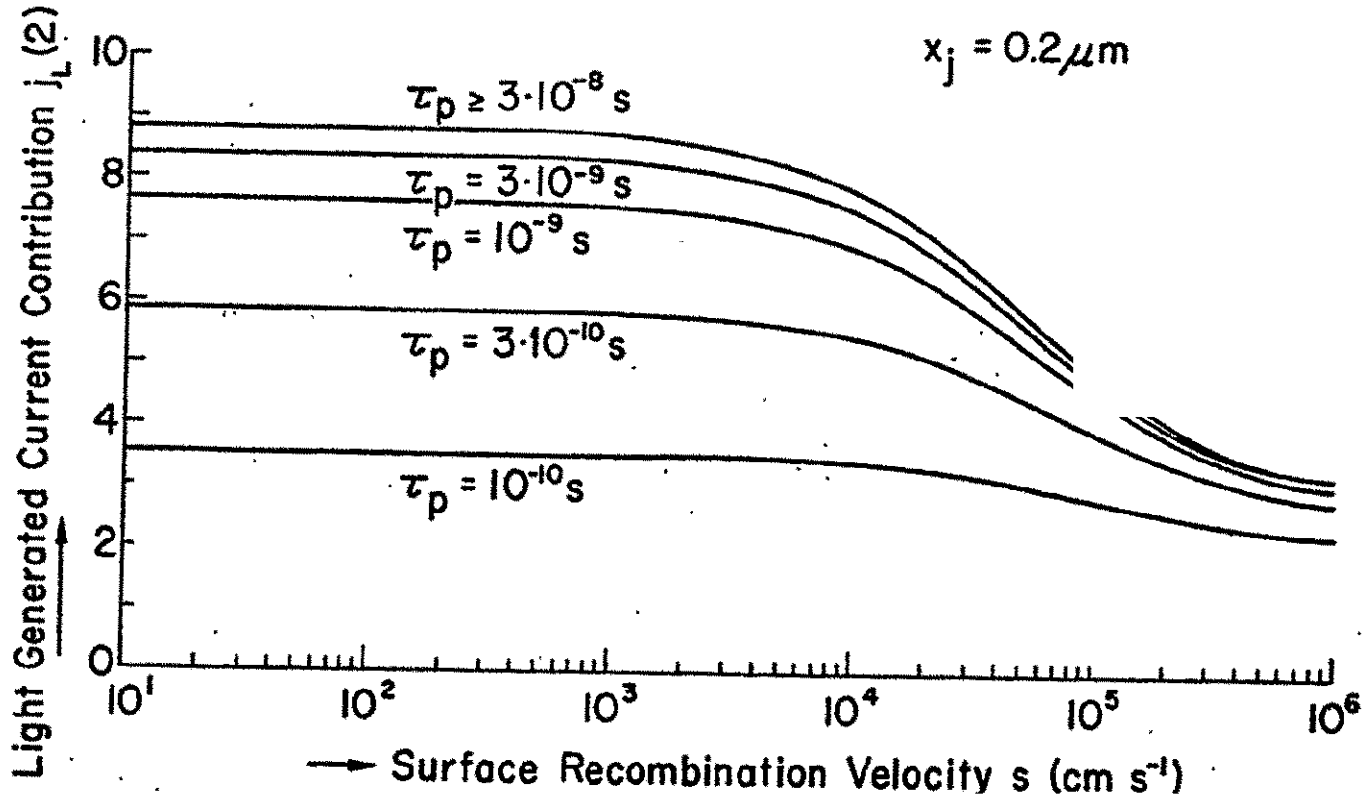

Fig. III-11 Short circuit current contribution from the diffused region as function of surface-recombination velocity, for several values of minority carrier lifetime τ_p.

With Fig. III-12, the discussion moves towards solar cells with greater thickness of the diffused region. This figure presents a plot of collection efficiency as function of wavelength for a diffused region thickness of 0.8 μm and a minority carrier lifetime of 0.3 μm, with surface recombination velocity as parameter. The plot is basically similar to the corresponding previous ones for 0.4 and 0.2 μm junction depth, but it is very evident that the diffused region plays a larger role in the collection process for the entire cell here than in the case of diffused regions of lesser thickness. Also, high surface recombination velocities have a more damaging influence on the entire collection efficiency curve than with thinner diffused regions.

The same observation can be made relative to the minority carrier lifetime which is used as parameter in a similar plot with constant surface recombination velocity of 100 cm s^{-1} (Fig. III-13). These last two figures make it obvious why, in view of the existing low values of minority carrier lifetime and large surface recombination velocity, the tendency was to develop devices with thinner and thinner diffused regions. However, Fig. III-13 also indicates that with a minority carrier lifetime of 30 μs -- only a factor of ten larger then observed on present solar cells-- and with considerably improved surface recombination velocity, cells with a 0.8 μm diffused region can be made with practically as good a collection efficiency as was postulated in ref. 1 for a diffused region of 0.2 μm thickness. Fig. III-14 shows the contribution of the diffused region to the light generated current as function of minority carrier lifetime, for a constant value of surface recombination velocity. This value was chosen sufficiently low to eliminate its influence. Again, most of the transition from large values of light generated current contribution to small ones takes place within 2 orders of magnitude of the minority carrier lifetime. However, this transision

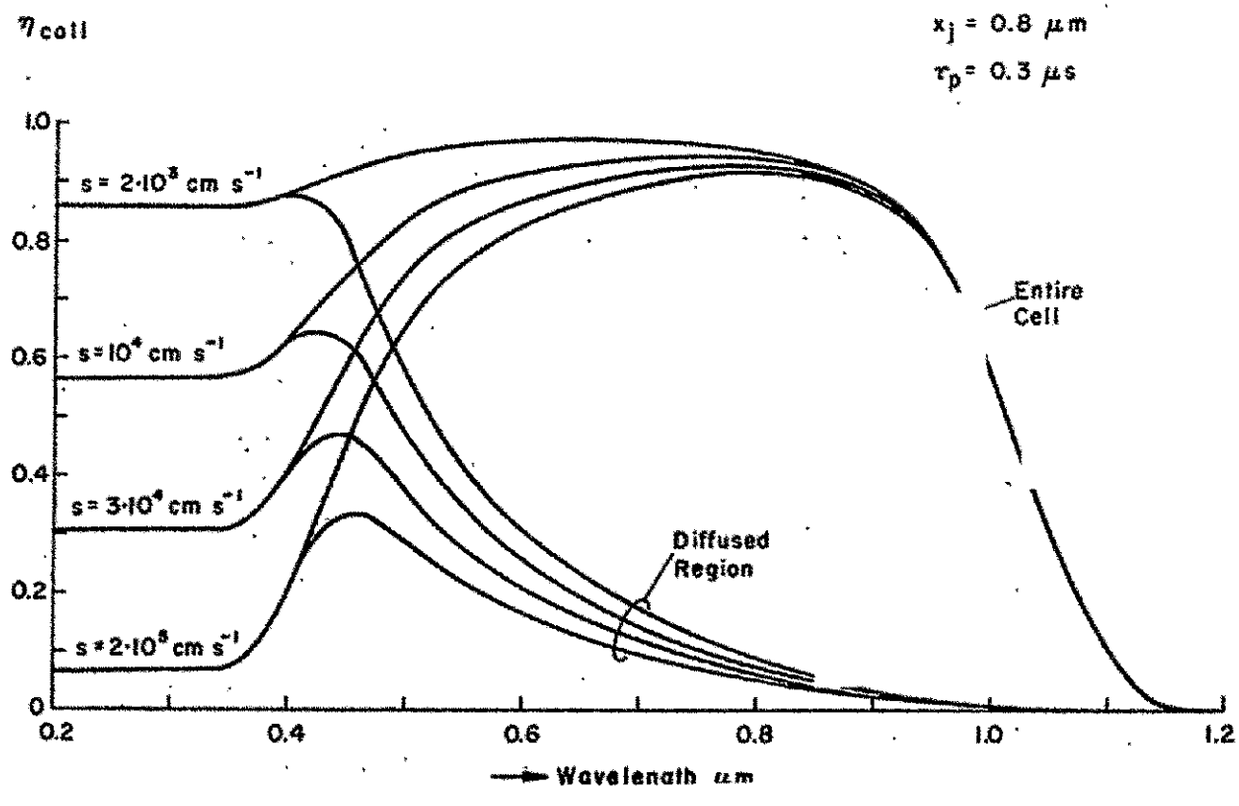

Fig. III-12 Collection efficiency as a function of wavelength from a diffused region of thickness x_j = 0.8 μm with a minority carrier lifetime τ_p of 0.3 μs, for several values of surface recombination velocity s.

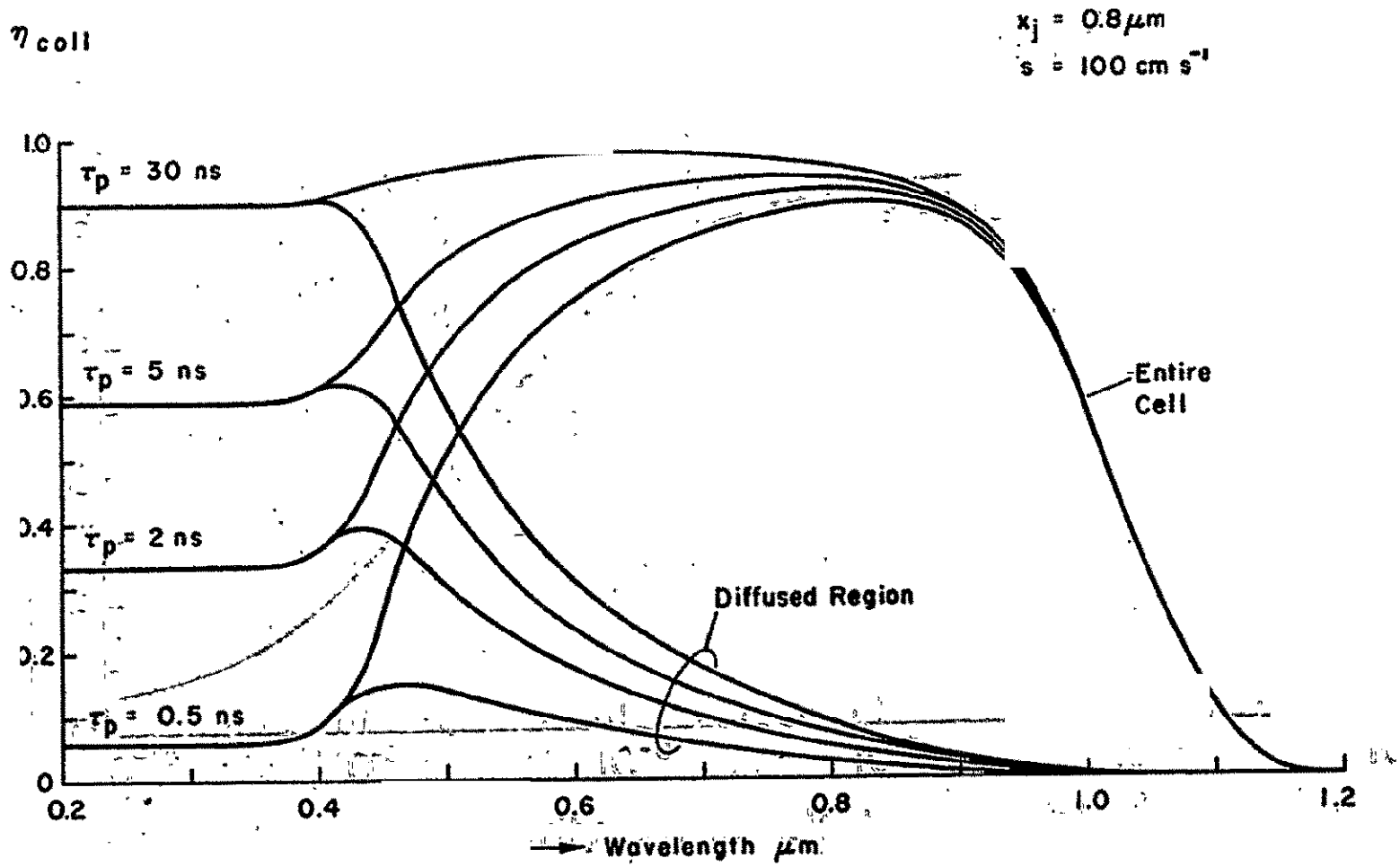

g. III-13 Collection efficiency as function of wavelength f values of minority carrier lifetime τ_p, with surface recombination velocity s = 100 cm s^{-1}.

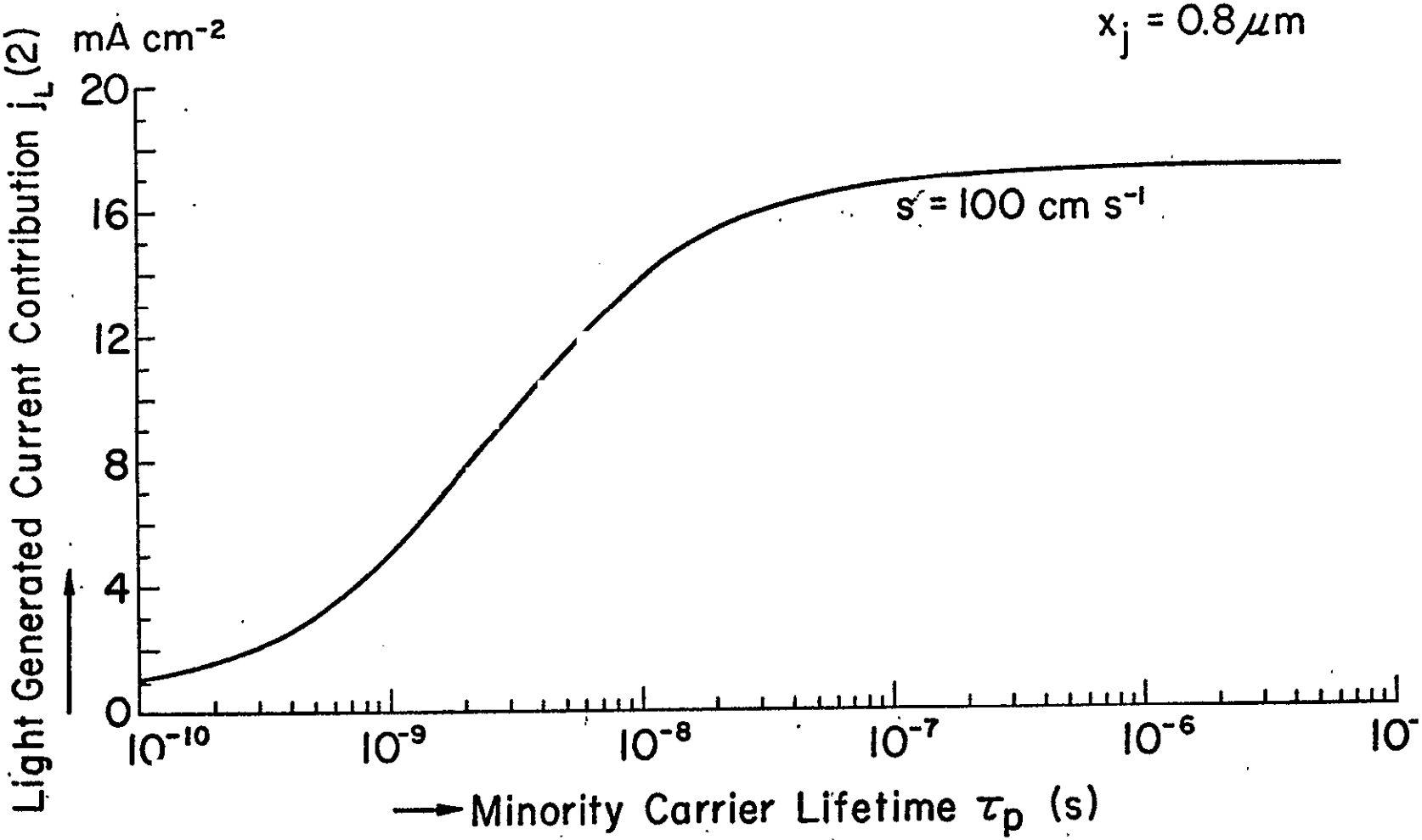

Fig. III-14 Short circuit current contribution from the diffused region as function of minority carrier lifetime, for a diffused region thickness $x_j = 0.8\ \mu m$.

region is shifted towards longer values of this lifetime, compared to the cells with thinner diffused regions. Fig. III-15, finally, shows the light generated current contribution from the diffused region of 0.8 μm thickness as function of surface recombination velocity, with minority carrier lifetime as parameter.

Numerous additional data were obtained, not only for the values of diffused region thickness discussed so far, but also for a thickness of 1.6, 2.5, and 6.4 μm. The latter two values of thickness were studied particularly in connection with the minority carrier lifetime of 4 μs which had been found desirable from consideration of the current-voltage characteristic. The presentation of all data would lead well beyond the scope of this report. However, these data are incorporated in the following figures and discussions. At 4 μs minority carrier lifetime, the diffusion length is approximately 20 μm. This is, for a diffused region thickness of 2.5 μm, 8 times the thickness value, and approximately three times the thickness value for the 6.4 μm thick diffused region. At the 2.5 μm thickness, the ideal short circuit current contribution from the diffused region can still be obtained with this value of minority carrier lifetime. However, the 6.4 μm thick diffused region can only deliver about 91% of the ideal light generated current contribution, if a surface recombination velocity of 100 cm s^{-1} is used.

Although an increase of the minority carrier lifetime proportional to the square of an increase in the diffused region thickness would be an expected requirement to achieve comparable performance, a dependence of performance on the surface recombination velocity relative to diffused region thickness variations is not obvious. Figure III-16 presents therefore the normalized light generated current contribution as function of surface recombination velocity for different diffused regions. The curves of this figure are plotted as function of surface recombination velocity for diffused region thickness of 0.2, 0.8, 2.5 and 6.4 μm. For each diffused

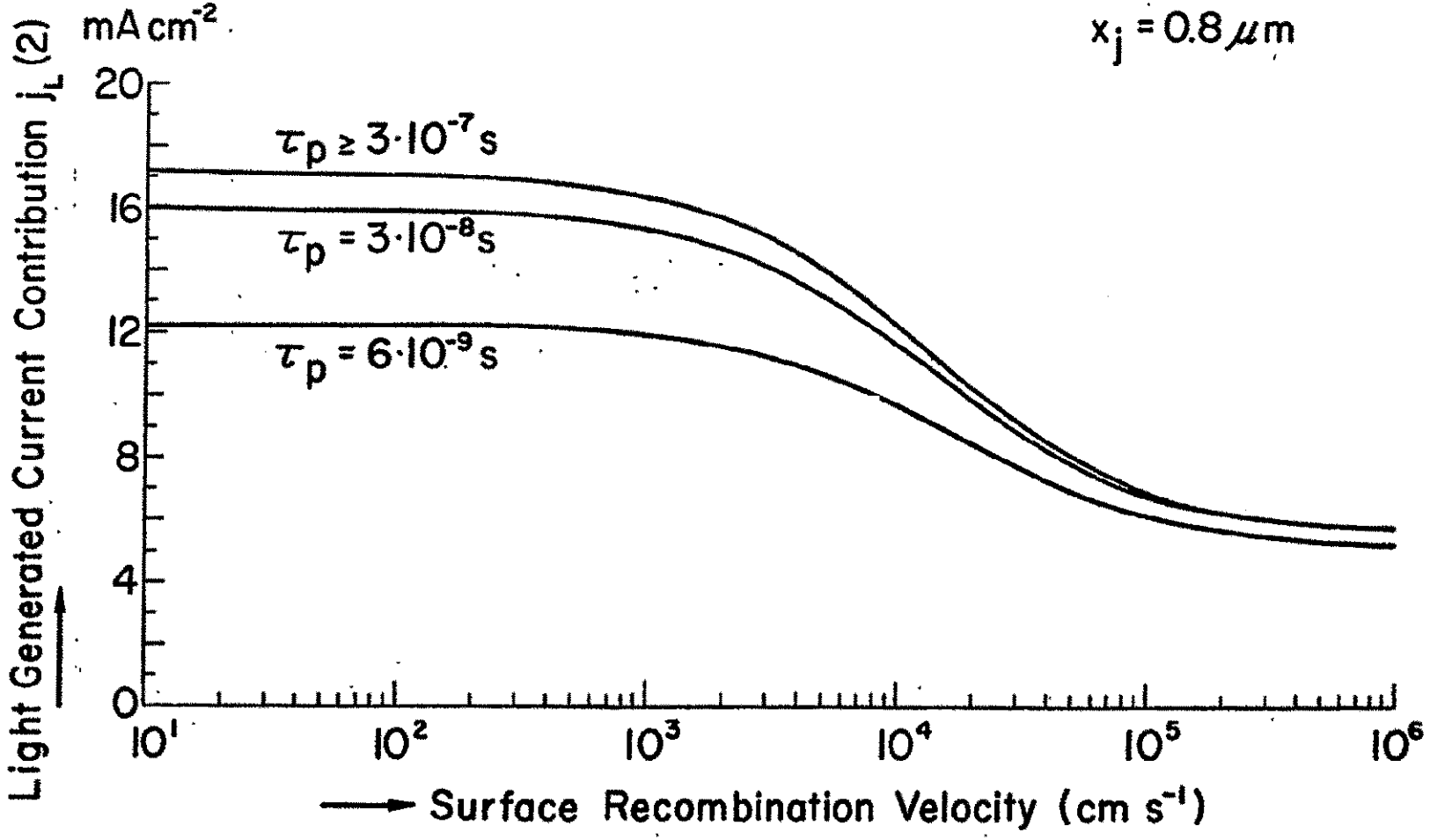

Fig. III-15 Short circuit current contribution from the diffused region as function of surface recombination velocity, for several values of minority carrier lifetime τ_p.

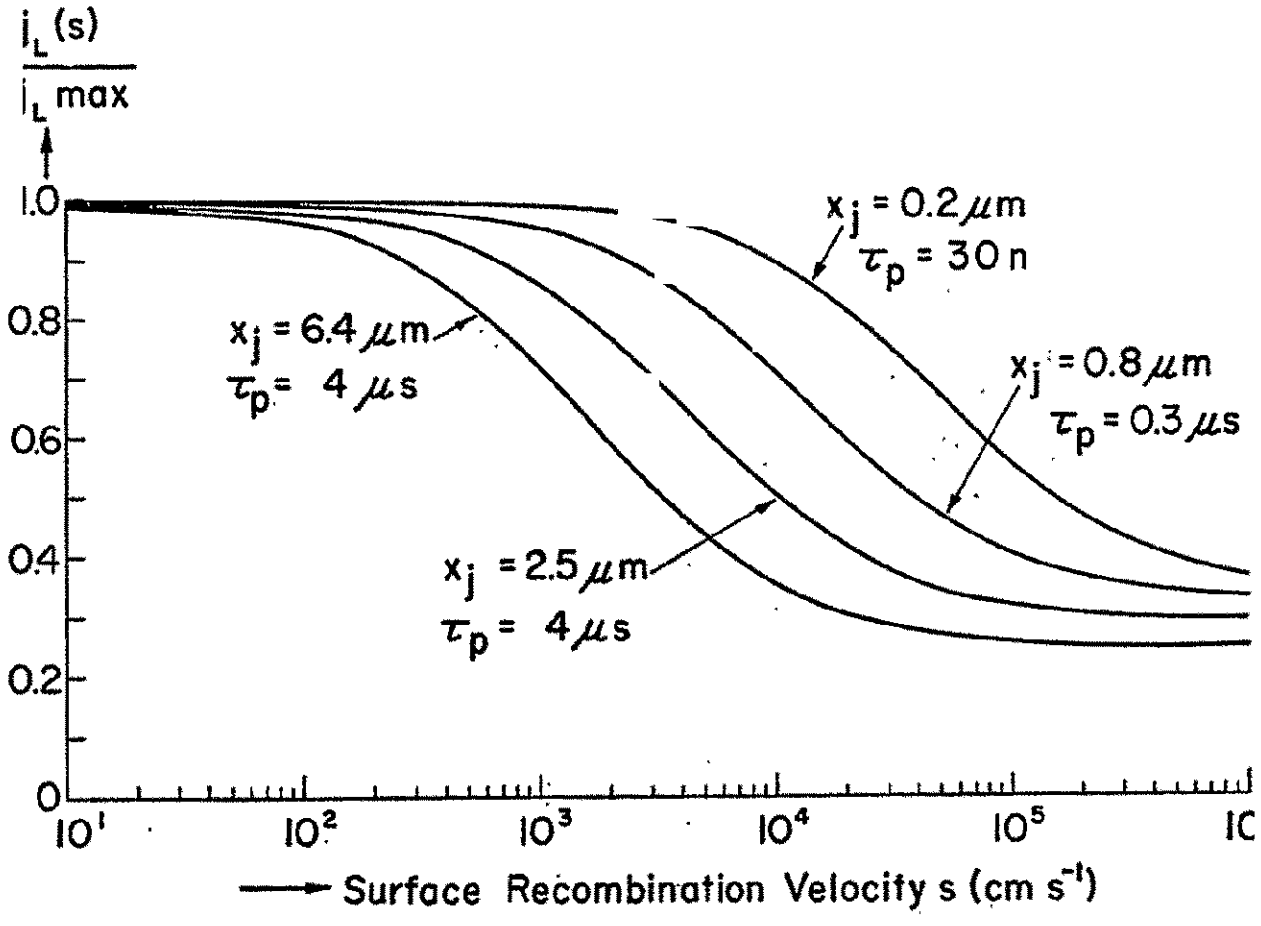

Fig. III-16 Normalized short circuit current contribution from the diffused region as function of surface recombination velocity, for several values of diffused region thickness x_j with minority carrier lifetime values τ_p which yield maximum light generated current.

region thickness, a minority carrier lifetime value has been chosen so that it falls well inside the saturation region, that is, above the value for which further increases in minority carrier lifetime will not yield higher values of light generated current. This statement holds for all curves except the one for a diffused region thickness of 6.4 μm, for which the minority carrier lifetime is close to reaching the saturation value. Since a diffused region of different thickness contributes a different amount of light generated current, the curves were all normalized to the maximum light generated current achievable under the airmass zero sunlight spectrum at a given thickness and with sufficiently large values of minority carrier lifetime and low surface recombination velocity. Figure III-16 illustrates clearly that the curves of normalized light generated current versus surface recombination velocity are of similar shape for varying diffused region thickness, but that they are displaced towards lower values of surface recombination velocity for the greater values of diffused region thickness. This statement about similarity holds at least down to a value of about 0.6 in normalized light generated current. As a matter of fact, one will observe that the product of surface recombination velocity and diffused region thickness is approximately constant down to the mentioned 0.6 value of normalized light generated current.

A solar cell designer will find himself confronted with questions such as: "If I want to approach the ideal light generated current within a given percentage, what values of minority carrier lifetime and surface recombination velocity should I strive for at a given thickness of the diffused region?" Curves to give answers to such questions are presented in Fig. III-17. Given are two sets of three curves each. One pair of curves applies for the case where 97.5% of the maximum possible light generated current contribution from the diffused region is to be obtained through choice of the corresponding parameter according to the applicable curve. The other

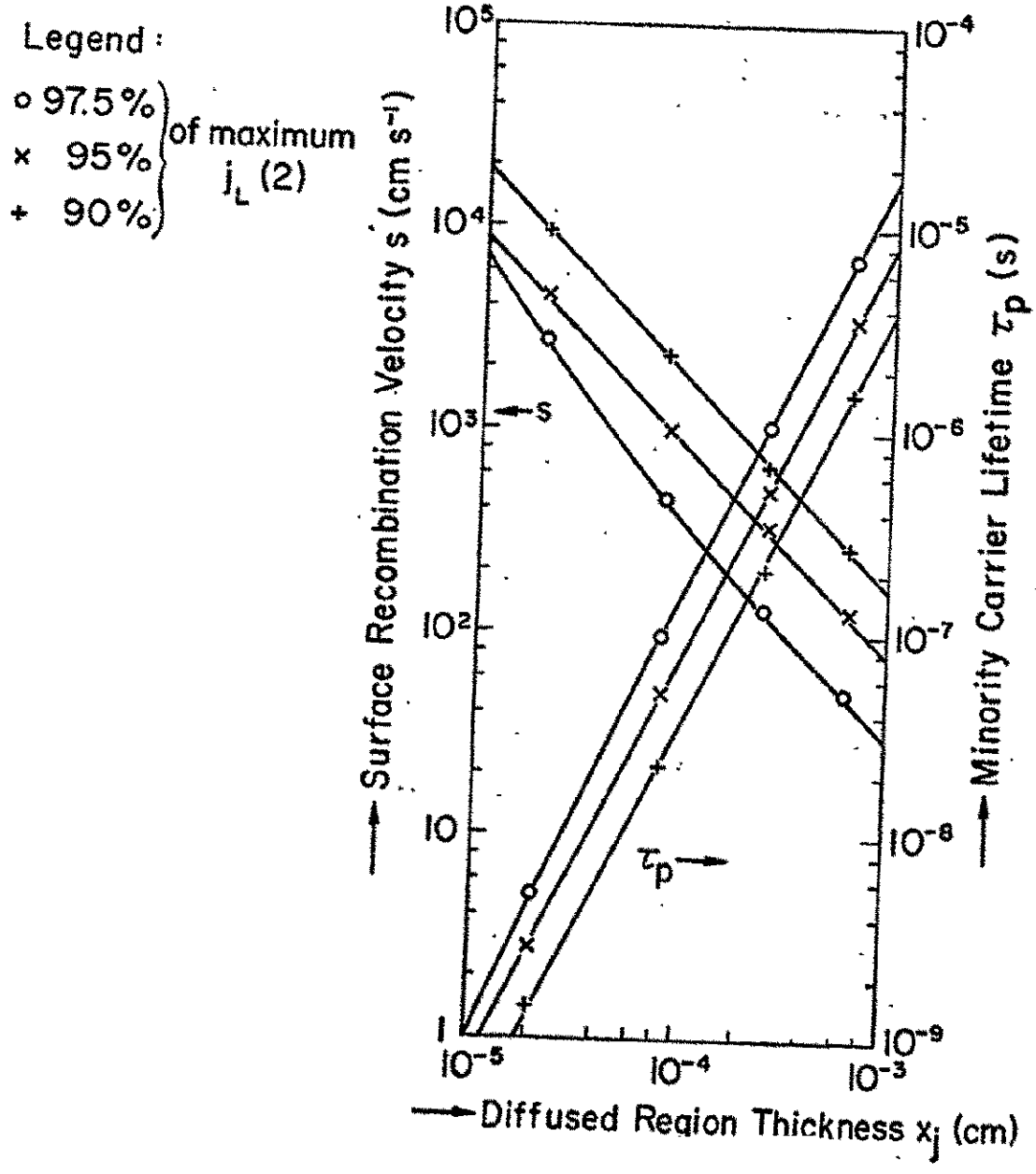

Fig. III-17 Design [illegible] parameters as function of the diffused region thickness. The curves yield the values of minority carrier lifetime τ_p and surface recombination velocity s, for which a short circuit contribution of 97.5%, 95%, and 90%, respectively, of the ideal can be obtained, assuming the other one of these 2 parameters being adjusted so that this is possible.

two pairs of curves apply for 95 and 90%, respectively, of the maximum light generated current contribution. Thus if values for minority carrier lifetime and surface recombination velocity are chosen from the 97.5% curves, a short circuit current contribution equal to approximately 95% (0.975 x 0.975) of the ideal case is expected to be obtained. It may be interesting to note that the curves for 90 and 95% of maximum light generated current contribution are straight lines on the log-log plot, and are parallel to each other. However, the curves for the 97.5% approach to the ideal case are curved. They indicate a requirement for higher perfection in both minority carrier lifetime and surface recombination velocity at the higher values of diffused region thickness.

3. Conclusions

A number of interesting conclusions can be drawn from the computations which were carried out to investigate the influence of material and device dimensional parameters on the performance of the diffused region. They are:

1. Present silicon solar cells operate at inadequate values of diffused region minority carrier lifetime and surface recombination velocity.

2. In order to improve device performance in view of the inadequacies mentioned above, the device developer is forced to move in the direction of decreased diffused region thickness.

3. Near ideal light generated current contributions from the diffused region should be achievable in the near future through proper choice of diffused region thickness, minority carrier lifetime, and surface recombination velocity without requiring great technological breakthroughs.

4. Technological breakthroughs in material processing should lead, in the long run, to the availability of longer minority carrier lifetimes in low resistivity silicon.

5. With values of minority carrier lifetime and surface recombination velocity, which are expected to be available later, larger values of diffused region thickness will become practical. The upper limit for the thickness probably will be near 6.4 μm. In order to protect the device from degradation due to radiation effects on spacecraft, the largest values of diffused region thickness will probably not be chosen.

6. Devices with lower values of diffused region thickness are more tolerant to lower values of minority carrier lifetime and of larger surface recombination velocities. Diffused regions of greater thickness carry a larger share of the minority carrier collection from the entire cell. Therefore, cells with large diffused region thickness will degrade more rapidly with deterioration of either diffused region minority carrier lifetime or surface recombination velocity.

4. References to Section III

Ref. 1

M. Wolf, "A New Look at Silicon Solar Cell Performance", Conference Proceedings of the 8th Photovoltaic Spacialists Conference, pp. 360 - 371, Aug. 4 - 6, 1970, Seattle, Wash. To be published in Energy Conversion, Pergamon Press.

Ref. 2

E.L.Ralph, "Performance of Very Thin Silicon Solar Cells", Conference Record of the 6th IEEE Photovoltaic Specialists Conference, pp. 98 - 116, Cocoa Beach, Fla., March 28 - 30, 1967

IV. Evaluation of Experimental Current-Voltage Data

1. Introduction

It is frequently necessary or desirable to describe the junction current-voltage characteristic of diodes or solar cells by a mathematical expression. Such need arises in device development efforts, in radiation effects studies, and in applications problems.

A mathematical model of the form:

$$I_D = I_0 \left[\exp \left(\frac{qV_D}{AkT} \right) - 1 \right] ; \qquad (1)$$

has commonly been used for this purpose.

Here, I_D and V_D are the junction current and voltage respectively, and I_0 is the saturation current. T is the absolute temperature, q and k are the electronic charge and the Boltzmann constant, respectively, while A is a dimensionless factor, originally introduced to better describe the experimental data.

With A = 1, equ. (1) represents the expression derived by Shockley for the pn junction diode based on the diffusion of thermally generated minority carriers (ref. 1). With $1 < A \leq 2$, it approximately describes the junction model including minority carrier generation in the depletion region as described by Sah-Noyce-Shockley (ref. 2).

In praxis, the terminal current I and the terminal voltage V are generally measured rather than the junction values. It is:

$$V_D = V - I R_s ; \qquad (2)$$

where R_s is the series resistance, assumed to be of the single lumped element form, and, in diodes:

$$I = I_D + \frac{V_D}{R_{sh}} \qquad (3)$$

where R_{sh} is the shunt resistance, representing ohmic shunt paths. In many practical devices, R_{sh} is sufficiently large so that this term can be neglected. The assumption

$$R_{sh} \rightarrow \infty ; \tag{4}$$

will therefore be made for the following work.

In solar cells and photodiodes:

$$I = I_D - I_L ; \tag{5}$$

where I_L is the light generated current. Note that $I_D \leq I_L$ in most operating modes of practical interest, so that $I \leq 0$.

It has been found, however, that equ. (1) does not describe the experimentally determined solar cell characteristics very well, but that a relationship of the form:

$$I_D = I_{01} \left[\exp \left(\frac{qV_D}{A_1 kT} \right) - 1 \right] + I_{02} \left[\exp \left(\frac{qV_D}{A_2 kT} \right) - 1 \right] ; \tag{6}$$

provides a much better description (ref. 3). The same appears to be the case with some diodes (ref. 4).

Five constants, I_{01}, A_1, I_{02}, A_2, and R_s (included in V_D) are thus required to uniquely describe the junction current-voltage characteristic.

In the past, these constants have been determined by plotting the experimental data on semi-logarithmic graph paper, correcting, when terminal data were plotted, the high-current points for the series resistance effect by use of a separately determined value for R_s, and drawing 2 best-fitting (visually !) straight lines through the data points.

The slopes of the straight lines provided the "A" - factors, their intersects with the ordinate the I_0 values. Successive approximation through checking the points in the overlap region between the 2 exponentials at intermediate voltage levels and in the transition region at small voltages, where the -1 terms become influential, against the experimental data has occasionally been used to improve the quality of the results.

It would be clearly desirable to replace this tedious method by a computer operation. Several attempts at this have been made in the past by other workers, who, however, used the single exponential expression (equ. 1) and achieved less than satisfactory results. A new approach to the problem was therefore indicated.

2. A Method for Numerical Evaluation of the IV Characteristic

The following describes a way to arrive at the values of the constants I_{01}, A_1, I_{02}, and A_2 for equ. (6) by a numerical method which lends itself to computer application. For this purpose, a set of at least 4 points on the current voltage characteristic obtained from experimental measurements is required. If R_s is not entered - the preferred approach -, then R_s will also be determined, requiring at least 5 measured points. For accuracy, however, a minimum of 12 points with junction current between 10^{-6} A cm^{-2} and 10^{-1} A cm^{-2} should be used.

There exist, basically, two approaches to obtaining the constants in an analytical description for a set of experimental data, after the type of the mathematical relationship (i.e. polynomial, exponential, etc.) has been determined. The first approach uses a set of data points equal in number to the number of constants to be determined for the mathematical relationship. The method provides a perfect fit to these data points. However, if a larger number of data points is available, no attention is paid to these points, nor to the quality of fit of the resulting mathematical relationship to these other points. The second approach, the least squares method (ref. 5),

provides those values for the constants for which the mathematical relationship provides the best ("most probable") description of all the data points entered into the evaluation, although possibly none of the points may lie exactly on the theoretical curve. The method is based on the assumption that the deviations follow the Gaussian error function. Since the attributes of the least squares method appear so much more appropriate to the problem at hand, this method has been selected for use.

Let $$I_k = f(V_k), \qquad k = 1, \ldots, n \tag{7}$$

be the n data points. Then their deviations from the theoretical relationship

$$I_D = f(V_D); \tag{8}$$

are:

$$v_k \equiv \tilde{I}_k - I_k ; \tag{9}$$

where $\tilde{I}_k$ are the values of I_D obtained by substituting $V_D = V_k$ into equ. (8), or, actually, equ. (6). According to the Gaussian law of error, the probability of obtaining the observed values I_k is:

$$P = \left(\frac{h}{\sqrt{\pi}}\right)^n \exp\left(-h^2 \sum_{k=1}^{n} v_k^2\right); \tag{10}$$

Clearly, a minimum of $\sum_k v_k^2$ will provide a maximum of P. Since the sum $S = \sum_{k=1}^{n} v_k^2$ is a function of the choice of the r constants $a_1, a_2, \ldots a_r$ in equ. (8), it follows that necessary conditions for a minimum are:

$$\frac{\partial S}{\partial A_1} = 0 ; \frac{\partial S}{\partial A_2} = 0 ; \ldots . \frac{\partial S}{\partial A_r} = 0 ; \tag{11}$$

Each "residual" v_k is a function of all constants a_i. Equ. (11) provides a set of r equations for r unknowns. This set consists of linear equations and is readily solvable in the case where equ. (8) represents a polynomial. If equ. (8) represents a function such that the set of equations according to equ. (11) is nonlinear, a good approach is to express equ. (8) by a Taylor series in the "constants" a_i, expressing the latter as

$$a_i = \tilde{a}_i + \Delta a_i \; ; \tag{12}$$

where the $\tilde{a}_i$ are estimated values of the constants a_i. Since the a_i's are constant, it is

$$\partial a_i = \partial \, (\Delta a_i) \; ; \tag{13}$$

Then:

$$f \, (V_D, \, a_1, \, a_2, \, \ldots . \, a_r) = f \, (V_D, \tilde{a}_1, \tilde{a}_2, \, \ldots . \tilde{a}_r)$$

$$+ \sum_{i=1}^{r} \frac{\partial f}{\partial a_i} \Bigg|_{a_i = \tilde{a}_i} \Delta a_i$$

$$+ \frac{1}{2!} \sum_{i,j=1}^{r} \frac{\partial^2 f}{\partial a_i \, \partial a_j} \Bigg|_{\substack{a_i = \tilde{a}_i \\ a_j = \tilde{a}_j}} \Delta a_i \, \Delta a_j$$

$$+ \ldots . \; ; \tag{14}$$

Assuming that the $\tilde{a}_i$ have been chosen so that tne Δa_i are sufficiently small, then equ. (14) can be broken off after the first order term, to obtain $\tilde{I}_k$. Then:

$$\frac{\partial S}{\partial a_i} = \frac{\partial \sum_{k=1}^{n} v_k^2}{\partial (\Delta a_i)}$$

$$= 2 \sum_{k=1}^{n} v_k \frac{\partial v_k}{\partial (\Delta a_i)} ;$$

$$= 2 \sum_{k=1}^{n} (\tilde{I}_{Dk} - I_{Dk}) \frac{\partial \tilde{I}_{Dk}}{\partial (\Delta a_i)} = 0 \quad i = 1,2, \ldots, r ; \quad (15)$$

According to equ. (6) :

$$\tilde{a}_1 = \tilde{I}_{01} ; \tilde{a}_2 = \tilde{B}_1 = \frac{q}{\tilde{A}_1 kT} ; \tilde{a}_3 = \tilde{I}_{02} ; \tilde{a}_4 = \tilde{B}_2 = \frac{q}{\tilde{A}_2 kT} ;$$

$$\tilde{a}_5 = \tilde{R}_s ; \quad (16)$$

and, with equ. (14):

$$\tilde{I}_{Dk} - I_{Dk} = \tilde{I}_{01} \left[\exp (\tilde{B}_1 V_{Dk}) - 1 \right] + \tilde{I}_{02} \left[\exp (\tilde{B}_2 V_{Dk}) - 1 \right]$$

$$+ \left[\exp (\tilde{B}_1 V_{Dk}) - 1 \right] \Delta I_{01} + \tilde{I}_{01} V_{Dk} \exp (B_1 V_{Dk}) \Delta B_1$$

$$+ \left[\exp (\tilde{B}_2 V_{Dk}) - 1 \right] \Delta I_{02} + \tilde{I}_{02} V_{Dk} \exp (\tilde{B}_2 V_{Dk}) \Delta B_2$$

$$- I_k \left\{ \tilde{I}_{01} \tilde{B}_1 \exp (\tilde{B}_1 V_{Dk}) + \tilde{I}_{02} \tilde{B}_2 \exp (\tilde{B}_2 V_{Dk}) \right\} \Delta R_s - I_{DK} = 0; \quad (17)$$

Also:

$$\frac{\partial \tilde{I}_{Dk}}{\partial (\Delta I_{01})} = \exp (\tilde{B}_1 V_{Dk}) - 1; \tag{18a}$$

$$\frac{\partial \tilde{I}_{Dk}}{\partial (\Delta B_1)} = \tilde{I}_{01} V_{Dk} \exp (\tilde{B}_1 V_{Dk}); \tag{18b}$$

$$\frac{\partial I_{Dk}}{\partial (\Delta I_{02})} = \exp (\tilde{B}_2 V_{Dk}) - 1; \tag{18c}$$

$$\frac{\partial \tilde{I}_{Dk}}{\partial (\Delta B_2)} = \tilde{I}_{02} V_{Dk} \exp (\tilde{B}_2 V_{Dk}); \tag{18d}$$

$$\frac{\partial \tilde{I}_{Dk}}{\partial (\Delta R_s)} = - \tilde{I}_k \left\{ \tilde{I}_{01} \tilde{B}_1 \exp (\tilde{B}_1 V_{Dk}) + \tilde{I}_{02} \tilde{B}_2 \exp (\tilde{B}_2 V_{Dk}) \right\}; \tag{18e}$$

Equ. (15) yields a system of r = 5 linear equations of the form:

$$C_{n1} \Delta I_{01} + C_{n2} \Delta B_1 + C_{n3} \Delta I_{02} + C_{n4} \Delta B_2 + C_{n5} \Delta R_s = C_{n6}$$
$$n = 1, 2, \ldots, r; \tag{19}$$

If R_s is predetermined, r = 4, and the C_{5n} terms are omitted.

Equ. (19) represents a system of 5 simultaneous linear equations which can be solved for the 5 unknowns by standard methods. The coefficients of these equations are then obtained from equ's (15), (17) and (18).

The computation of the coefficients and the evaluation of the set of simultaneous linear equations lend themselves readily to computer application.

3. A Computer Program for Determining the 5 Constants

The evaluation of the system of linear equations containing matrix elements C_{11} through C_{56} to obtain correction values to be applied to the set of estimated values for the 5 constants, is a straightforward task. So is the repeated application of this method to obtain a best fitting set of 5 constants.

However, it has been found that the method is very sensitive due to the exponential nature of the relationship (equ. 6), so that divergence can occur or that intermediate terms attain magnitudes exceeding the capacity of the computer. It has been found that different choice of estimated values or manipulation of the correction values or of intermediate terms overcomes the problem.

It would be clearly desirable to have a computer program which will always arrive at a set of constants which provide the best fit of the theoretical relationship to the experimental data, without any actions by the computer operator beyond entering the experimental data. This condition includes the requirement that a single set of estimated starting values will suffice to achieve convergence and arrive at the least squares approximation for any set of data entered. This feature is particularly useful when large amounts of data are to be reduced, which will be the case, for instance, in reduction of housekeeping or experimental data by telemetry from a spacecraft. Here, it would be particularly interesting to obtain a simple printout of the variation in time of the parameters of interest, without any manual reductions or computer manipulations required. A special effort has, therefore, been made to augment the basic program of the least squares method so that it will run through and come to a convergence without any operator influence. These additions have expanded the program considerably, but have fulfilled their task in the data reductions carried through as test cases so far.

In the effort to make the program self-running, it was found that the choice of the estimated value for the series resistance was particularly critical for achieving convergence. The program is arranged now so that, if convergence is not achieved, a different estimated value of resistance will be tried until convergence is achieved, or until the values of resistance are outside of reasonable bounds.

The program has been designed to be rather flexible, so as to permit different types of input data, as well as to provide different forms of output computations. The program will accept both solar cell current-voltage data and dark diode current-voltage data. Furthermore, the program will accept the data either in the form of junction data, that is, after the elimination of the influence of series resistance, or as terminal data including the effect of series resistance. If junction data are entered into the program, the problem consists only in the solution of 4 linear equations, and series resistance will not be contained in the output data. It is further possible to carry out the computations for a fixed value of the factor A_1, usually $A_1 = 1$. In the case of the evaluation of the parameters with a fixed factor A and no series resistance, the problem is reduced to the solution of 3 linear equations. Also, A values slightly below 1 have repeatedly been obtained. Since such A values are not expected to be physically meaningful, the program has been altered so as to provide in these cases the constants with $A_1 = 1$.

The printout of the program contains the saturation current I_{01} and the factor A_1 for exponential 1, the saturation current I_{02} and factor A_2 for exponential 2, and the final value R_s for the series resistance. Also, the standard deviation σ for all data points from the final theoretical curve, based on the computed constants, is printed out. It has been found that standard deviations near 5% are most commonly obtained. Such a value is very reasonable, since the experimental data have to be expected to contain errors of this magnitude.

It has been further observed that relatively small changes in the standard deviation are connected with changes in the 5 constants which might be considered meaningful. This is illustrated in Table IV-1. Here, the best-fit data obtained by the computer are compared with results obtained by the old manual method. Also, fixed values of R_s and of A_1 have been entered into the computer evaluation. It is evident, that changes in A and R_s by 5% and in I_{01} by 50% can be connected with a relative change in the standard deviation of + 10% (from 3.7% to 4.1%). This will have to be kept in mind by using these 5 constants in describing experimental data. To obtain higher confidence into the theoretical description of the current-voltage characteristic, it may ultimately become necessary to acquire more accurate experimental data. This last point leads to an interesting observation. The least squares method slavishly alters the constants for the theoretical expression, until the best fit to the experimental data has been found, that means, the smallest standard deviation is obtained. However, small changes in the standard deviation may be associated with "meaningful" changes in the theoretical parameters. It may be, however, questioned, in view of the quality of the data entered into the evaluation, whether it is reasonable to change the theoretical constants in order to reduce the standard deviation by a small amount. As an example, it had been observed from previous manual reduction of data on the I-V characteristics of silicon solar cells which had been subjected to nuclear particle radiation, that the five constants appeared to be changing in a certain fashion as a result of this irradiation. Evaluating the same data with the computer program however seems to result in a less orderly change of these constants. This leads to the interesting philosophical question: will it be possible to obtain meaningful results after substituting

TABLE IV-1

Values of the 5 Constants for Solar Cell D-9, Measured 4-7-70
After Irradiation with $3 \cdot 10^{15}$ cm^{-2} Electrons (1 MeV)
Determined Manually and by Computer with Different Input Data

Input Data		Output Data					
R_s	A_1	I_{o1}	A_1	I_{o2}	A_2	R_s	σ
Ω	-	A	-	A	-	Ω	%
V	V	$9.4 \cdot 10^{-10}$	1.07	$1.7 \cdot 10^{-6}$	3.25	0.816	3.7
0.76	V	$1.5 \cdot 10^{-9}$	1.10	$1.8 \cdot 10^{-6}$	3.38	-	4.3
0.78	V	$1.3 \cdot 10^{-9}$	1.09	$1.8 \cdot 10^{-6}$	3.33	-	3.9
0.80	V	$1.1 \cdot 10^{-9}$	1.08	$1.8 \cdot 10^{-6}$	3.28	-	3.7
0.82	V	$9.1 \cdot 10^{-10}$	1.07	$1.7 \cdot 10^{-6}$	3.24	-	3.7
0.84	V	$7.8 \cdot 10^{-10}$	1.06	$1.7 \cdot 10^{-6}$	3.20	-	3.8
0.86	V	$6.6 \cdot 10^{-10}$	1.04	$1.7 \cdot 10^{-6}$	3.16	-	4.0
0.88	V	$5.6 \cdot 10^{-10}$	1.03	$1.6 \cdot 10^{-6}$	3.13	-	4.4
V	1.00	$3.2 \cdot 10^{-10}$	-	$1.5 \cdot 10^{-6}$	2.98	0.893	5.2
Earlier Manual Reduction		$2.3 \cdot 10^{-10}$	1.0	$1.6 \cdot 10^{-6}$	3.0	1.0	-

V = Variable, determined by computer

a "dumb" computer for a "skilled" investigator as readily as before the substitution? It is obvious that the "skilled" investigator is liable to apply some "bias" in his interpretation of the data, that he may look for some relationships which may be very weak or not existent at all. On the other hand, this "bias" may also lead to the recognition of potential relationships which can be confirmed or disproved by further detailed or more accurate investigation. The computer would not apply a similar bias, and would give immediately objective results from the data entered into the evaluation. On the other hand, faint relationships may go undetected. Interestingly, this question is already touched upon in the discussion of the least squares method in ref. 5

The upshot of this last little discourse is, that caution has to be exercised in the use of data, and that the results have to be related to the quality of the experimental data. Objective results have ultimately to be obtained, be it through more accurate data or a greater data base, with statistical evaluation of error magnitude and degree of correlation. Since the usefulness of this computer program still has to be established through more extended application, a further description of the program and of its use will be postponed to the next semiannual report.

4. Conclusion.

A computer program has been developed for the description of the solar cell current-voltage characteristic by "best fit" from experimental data. The usefulness of the program still has to be proven through more extensive application.

5. References to Sect. IV

Ref. 1

W. Shockley, "Electrons and Holes in Semiconductors", pp. 309-318, Van Nostrand, New York, N. Y. 1954

Ref. 2

C. T. Sah, R. N. Noyce & W. Shockley
"Carrier Generation and Recombination in P-N Junctions and P-N Junction Characteristics"
Proc. IRE 45, pp. 1228-1243, Sept. 1957

Ref. 3

M. Wolf and H. Rauschenbach, "Series Resistance ------ on Solar Cell Measurements", Adv. Energy Conversion 3, pp. 455 - 479, Pergammon Press, 1963

Ref. 4

H. Queisser, private communication

Ref. 5

I. S. Sokolnikoff and E. S. Sokolnikoff, "Higher Mathematics for Engineers and Physicists", pp. 536 - 544, McGraw-Hill, New York, N. Y., 1941

V. Project Status

In section 1 of the work schedule "Optimum Device Structure", points a (Determine diffused region parameter interrelation) and b (Determine base region parameter interrelation) are completed.

Work on points 1c, 2a, and 2b has been started.

VI. Plans for the Next reporting period.

Shift prime emphasis to reduction of surface recombination velocity (section 2 of work schedule), with simultaneous progress on point 1c, including completion of work on the computer program.